

DRAFT

ARGONNE NATIONAL LABORATORY
9700 South Cass Avenue, Argonne, Illinois 60439

Analysis of Flow Stratification in the Surge Line of
the COMANCHE PEAK Reactor

by

J. G. Sun, Y. H. Shen, and
W. T. Sha

Materials and Components Technology Division
Analytical Thermal Hydraulics Research Program

January 1991

9101230332 910114
PDR ADOCK 05000445
P PDR

Contents

Contents.....

1 Introduction.....

2 Objectives.....

3 Brief Description of the COMMLX Code.....

 3.1 Background.....

 3.2 Equations Solved.....

 3.3 Unique Features.....

 3.4 Other Features.....

4 Flow Stratification in a Surge Line.....

 4.1 Surge Line Layout of COMANCHE PEAK Reactor.....

 4.4.1 Initial Conditions.....

 4.4.2 Boundary Conditions.....

 4.2 Experimental Measurements.....

 4.3 Numerical Simulation Model Used in the COMMLX Code.....

 4.4 Initial and Boundary Conditions.....

 4.5 COMMLX Results.....

 4.6 Comparison of COMMLX Results with Measurements.....

5 Discussion and Conclusions.....

Acknowledgment.....

Reference.....

Executive Summary

Flow stratification is known to occur in various reactor components during normal and off-normal operating conditions of both PWR and BWR. Large temperature difference is normally associated with flow stratification. Thus, when flow stratification occurs in a reactor component, it will be subject to an additional thermal stress resulting from the local temperature difference. A number of nuclear power plants have reported failure of reactor components due to flow stratification. Flow stratification not only can cause reactor shut down due to unisolable leak resulting from failure of reactor component, but also has significant implications to reactor safety and can alter both the sequence and consequence of a reactor accident. Therefore, it is imperative to understand the causes of flow stratification and more importantly, we should be able to predict when and where flow stratification will occur and its magnitude of temperature difference associated with the flow stratification. The work presented here represents the first step in this direction and will contribute to the resolution of the issue of flow stratification.

An analysis is performed using the COMMLX-1C computer program for the surge line of COMANCHE PEAK reactor. The COMMLX-1C computer code is developed and sponsored by the Office of Nuclear Regulatory Research, United States Nuclear Regulatory Commission and is a three-dimensional transient single-phase computer program for thermal hydraulic analysis of single- and multicomponent engineering systems. It solves conservation of mass, momentum, and energy equations as a boundary value problem in space and an initial value problem in time domain and has been applied to flow stratification and natural circulation during postulated reactor accidents. The major objective of this work is to demonstrate that the COMMLX code is capable of predicting flow stratification. The numerical results obtained from the COMMLX code for the surge line of the COMANCHE PEAK reactor presented here have been compared with the measurements provided by the Westinghouse Electric Corporation and the agreement is good.

1 Introduction

Flow stratification results from density difference of two streams of a fluid or different fluids flowing at relatively low velocities with very little mixing. The density difference is

attributed either to temperature difference of two streams of a given fluid or different fluids with different intrinsic density. The scope of this study is limited to flow stratification resulting from temperature difference of two streams of a given fluid. These two streams are flowing at low velocity with very little turbulent mixing between them. The lighter, hot fluid stays above, and the heavier, cold fluid stays below in a flow domain.

A number of nuclear power plants have reported failure of reactor components due to flow stratification.¹ The most common occurrences of flow stratification in reactor components during normal (including transients) and off-normal operating conditions are surge line, hot leg, RHR line, feed water line, steam generator feed water ring, etc. Flow stratification not only can cause reactor shut down due to unisolable leaks resulting from failure of reactor components, but also has serious implications of reactor safety. It has been shown² that flow stratification can occur in a hot leg and most likely in a surge line* during postulated TLMB accident (station blackout). One of the possibilities of failure of the pressure boundary due to flow stratification, prior to breach of the reactor vessel by molten core and should this failure occur early enough, the reactor system may depressurize sufficiently to avoid direct containment heating when the core debris is ejected following vessel failure. Thus, flow stratification can alter both sequence and consequence of a severe accident. Therefore, fundamental understanding of flow stratification is essential to avoid possible reactor shut down or leading to an undesirable reactor accident. The present work represents first step in that direction and will provide a reliable predictive capability of flow stratification in terms of when, where, and the magnitude of temperature difference. It is to be noted that flow stratification was not accounted for in the original design of all light water reactors (LWR) and it certainly has significant impact on life extension of all existing LWRs.

2 Objectives

The objectives of this study are:

* In this particular analysis, surge line was not explicitly included.

1. To demonstrate the capability of the COMMLX computer code capable of predicting flow stratification in various reactor components
2. To present results obtained from the COMMLX code for the surge line of COMANCHE PEAK reactor and to compare with the plant measured data.

3. A Brief Description of the COMMLX Code

The COMMLX code^{3,4,5} is a generalized computer code for heat transfer and fluid flow analysis. Its capabilities include steady-state/transient, three-dimensional, and single-phase analysis of nuclear reactor systems under normal and off-normal operating conditions. Recently, the COMMLX code has been and continues to be extended and modified to multiphase applications of various engineering systems.

COMMLX is a well-refined and -tested code. Already, a large number of computations have been performed for complex situations, and many organizations, both here in the U.S. and abroad, are using the code to simulate industrial problems. The structure of the code is modular. Its many unique features are described in the following.

3.1. Background

The development of COMMLX began in the summer of 1976. The initial version, COMMLX-1,³ was documented and made available to the public (through the U.S. Nuclear Regulatory Commission) in January 1978. The advanced version, COMMLX-1A,⁴ with more capabilities and flexibilities, was released in 1983. Developmental work continued to add improved models and to expand applications to non-nuclear systems. The extended version, COMMLX-1B, was released in December 1985. The latest version is COMMLX-1C,⁵ which was released very recently (September 1990). Many additional improvements have been incorporated into COMMLX-1C over COMMLX-1B.

3.2 Equations Solved

Three-dimensional, time-dependent conservation equations of mass, momentum, and energy and transport equations of turbulence parameters, along with the equation of state, are solved as a boundary value problem in space and an initial value problem in time.

The solution provides three-dimensional detailed descriptions of

- velocity,
- temperature, and
- pressure,

along with ancillary information such as heat transfer and resistance correlations. For easy interpretation, the numerical results can be transformed into graphic forms (e.g., vector plots, isotherm plots, and video or film showing fluid motion).

3.3 Unique Features

COMMIX Porous-Medium Formulation

COMMIX employs a new porous-medium formulation⁶ based on local volume-averaging. This formulation uses four parameters—volume porosity, directional surface porosity, distributed resistance, and distributed heat source (sink)—to model the effects of internal solid structures. In the conventional porous-medium formulation, only three parameters—volume porosity, distributed resistance, and distributed heat source—are used. The addition of a fourth parameter, directional surface porosity, is a new concept that greatly facilitates modeling of velocity and temperature fields in anisotropic media and, in general, improves resolution and accuracy.

Two Solution Algorithms

COMMIX has two solution algorithms for single phase systems that are provided as user's options:

- A semi-implicit algorithm derived from the Los Alamos ICE Technique.^{7,8,9} This algorithm is ideally suited for analyzing fast transients, where one is interested in details at small time intervals (on the order of Courant time step).
- A fully implicit algorithm names SIMPLEST-ANL.⁴ This algorithm is a modification of the Patankar-Spalding numerical procedure¹⁰ known as SIMPLE/SIMPLER. It is particularly suitable for the analysis of slow and normal transients.

These two solution procedures are combined into one formulation. But they are implemented so that a user can switch from one solution scheme to another at any time during a transient simulation of a problem.

The Geometry Package

The geometry package developed and implemented in COMMIX is capable of approximating any irregular geometry. It uses basic computational cells as building blocks to model the geometry under consideration. Then both volume porosities and directional surface porosities are used to account for the differences between the approximated and actual configurations.

To save computer storage, a computational cell is defined by a number rather than by its conventional (i, j, k) location, where i, j, and k are the computational cell indices in the three principal axes (e.g., x, y, and z in the Cartesian coordinate system). With this approach, the storage requirement depends only on the total number of computational cells and not on the dimensional values of (IMAX * JMAX * KMAX), where IMAX, JMAX, and KMAX denote the maximum values of computational cell indices in the three corresponding principal axes.

A normal three-dimensional computational cell has six surfaces. But to facilitate true and proper modeling of a complex irregular geometry (and most geometries in engineering systems are complex and irregular), we have provided flexibility so that a user can specify an additional seventh surface, called an irregular surface to a computational cell.

3.4 Other Features

Other features of COMMIX are described below.

- For single-phase applications, the following two turbulence model options are provided:
 - Constant turbulent diffusivity model.
 - Two-equation (k-ε) model where k is the turbulent kinetic energy and ε is the dissipation rate of k.
- A flow modulated skew-upwind difference scheme⁵ has been developed and implemented to reduce numerical diffusion, specifically for the case of flow inclined to grid lines.
- The final form of all of the sets of discretization equations is

$$a_0^* \phi_0 - \sum_{l=1}^6 a_l^* \phi_l - b_0^* = 0,$$

where ϕ is a dependent variable and the subscript l stands for neighboring points. This general form of the discretization equation lends itself to various solution schemes, e.g., SOR, Preconditioned Conjugate Gradient Method, and direct matrix inversion.

- The solution has a decoupled-transient-simulation option that permits solution of
 - mass-momentum equations only, or
 - energy equation only, or
 - coupled mass-momentum, and energy equations,
 at any given time step.
- The code has an option that allows use of either Cartesian or cylindrical coordinates.
- COMMIX has built-in properties for liquid sodium and water, with an option permitting use of simplified property correlations for any fluid.

- The code also contains:
 - A generalized resistance model to permit specification of resistance due to internal structures (fuel rods, wire wrap, baffles, grid spacers, etc.).
 - A generalized thermal structure formulation to model thermal interaction between structures (fuel rods, wire wraps, duct wall, baffles, etc.) and surrounding fluid.
- Heat source/sink and boundary conditions can be functions of time.
- The COMMIX code is structured to permit solution of one-, two-, or three-dimensional calculations.

4 Flow Stratification in a Surge Line

A detailed three-dimensional and time-dependent analysis is performed using the COMMIX-1C code for the surge line of the COMANCHE PEAK reactor. Temperature distributions of both fluid and surge line wall are calculated. First, the surge line layout of the COMANCHE PEAK reactor will be described, the experimental measurements provided by Westinghouse¹¹ is presented, the numerical model used in the COMMIX calculation is outlined, both initial and boundary conditions based on the limited measurements used in the COMMIX code are followed. Finally, the detailed velocity profiles and temperature distributions of the surge line obtained from the COMMIX code are presented and compared with the experimental measurements.

4.1 Surge Line Layout of COMANCHE PEAK Reactor

Figure 1 presents the layout of the surge line of the COMANCHE PEAK reactor. All pipe dimensions and pipe outside and inside diameters are shown in Fig. 1. The temperature monitoring locations, namely T1, T2, T3, and T4 are also shown in Fig. 1. These temperature monitors record the outside pipe wall temperature at various circumferential locations.

4.2 Experimental Measurements

Figures 2-5 are temperature measurements as a function of time of T1, T2, T3, and T4 respectively, at the various circumferential locations. Temperatures as a function of time of the four hot legs are shown in Fig. 6, the hot leg marked 4 in Fig. 6 is the hot leg with the pressurizer. The water level of the pressurizer as a function of time is marked 7 in Fig. 7. Figure 7a is the enlarged view of a portion of Fig. 7. The relationship between the water level height of the pressurizer versus volume is presented in Table I.

4.3 Numerical Simulation Model Used in the COMMIX Code

The numerical model simulates the surge line of the COMANCHE PEAK reactor are shown in Figs. 8-10. The computational mesh set up along the pipe line is shown in Fig. 8. Figure 9 presents the typical cross section of the surge line and the typical elbow is modeled as shown in Fig. 10. In order to avoid modeling complications, the pipe marked L1 in Fig. 1 is modeled as a vertical run as shown in Fig. 8. This simplification will not affect the results and will be discussed in Sec. 5.

The heat capacity effect of the surge line is explicitly accounted for in the numerical calculation. The wall thickness is equally divided into two computational grids in the numerical model and the thermal physical properties of pipe wall used in the COMMIX calculations are as follows:

$$\rho \text{ (density)} = 7977 - 0.4167 T \text{ (kg/m}^3\text{)}$$

$$k \text{ (thermal conductivity)} = 14.16 + 0.0131 T \text{ (W/m-}^\circ\text{C)}$$

$$C_p \text{ (specific heat)} = 508.67 \text{ (J/kg-}^\circ\text{C)}, \text{ and}$$

$$T \text{ (temperature) in } ^\circ\text{C}.$$

4.4 Initial and Boundary Conditions

A close examination of the experimental measurements as shown in Figs. 2-5 reveals that flow stratification with large temperature difference took place approximately from 17 1/2 hours to 21 1/2 hours in the transient. One of the objectives of this work is to

demonstrate the capability of the COMMIX code to analyze flow stratification. Consideration is also given to save computer running time. It is thus decided to start our calculation at 17 hr, 31 min, and 10 sec in the transient. Since we do not start our calculation at the very beginning of the transient, the initial condition corresponding to the beginning of our calculation must be constructed. Also the boundary conditions as a function of time at the inlet of the surge line (from the hot leg to surge line) must be provided. Both initial and boundary conditions used in the COMMIX calculation will be described below.

4.4.1 Initial Conditions

- Velocity distribution based on isothermal steady-state solution with inlet velocity of 0.002 m/s at the inlet of the surge line (from hot leg to surge line).
- The outside pipe wall temperature distribution of all horizontal pipes (L2 and L3) based on T2 and T3 readings and linearly interpreted and extrapolated both axially (along the pipe length) and circumferentially. The outside pipe wall temperatures in L1 and L4 are assumed to be uniformly distributed according to T1 and T4 readings respectively. All fluid temperature next to the pipe wall of L2 and L3 are assumed to be the same and they are stratified. Temperatures in L1 and L4 are assumed to be uniform at 152.6°F (see Fig. 6) and 440F (same as surge line wall temperature, Fig. 5), respectively. It is to be noted that the assumption of uniform fluid temperature in L1 and L4 is reasonable since both T1 and T4 readings after we started the calculation appear to support the assumption.

4.4.2 Boundary Conditions

- At the inlet of surge line (from hot leg to surge line)

-Inlet velocity based on the water level of pressurizer (Fig.7) as shown in Fig. 11.

Figure 11 is obtained in the following manner.

Since water is an incompressible fluid, its level change in the pressurizer is directly related to the water flow rate from the surge line to the pressurizer.

which in turn, related to the flow rate from the hot leg to the surge line. Therefore, the instantaneous mean inlet water velocity v_{in} is evaluated from

$$v_{in} = \frac{QdH}{A dt}$$

where H is the water level in the pressurizer (in %) as shown in Fig. 7, Q is the volume of the water in gallons in each percent change of the pressurizer level as shown in Table 1. A is the cross sectional area of the surge line pipe, and t is the time. It is seen from the above equation that the inlet velocity is proportional to the slope of the water level change in the pressurizer as a function of time. When the experimental data of Fig. 7 for the water level (in %) was enlarged by many times (see Fig. 7a), it can be seen that the slope becomes positive from about 17 hr 31 min, and it increases to a maximum after about 17 hr 36 min. Then the slope decreases and comes back to another maximum, after which it gradually declines and eventually the slope reaches to very small value. The inlet velocity follows the same pattern as shown in Fig. 11.

-Inlet temperature based on the outside pipe wall temperature reading of the hot leg (nearby the surge line) with pressurizer (Fig. 6) as shown in Fig. 12.

- At the outlet of surge line (from surge line to pressurizer):

$$\frac{\partial v}{\partial x} = \frac{\partial T}{\partial x} = 0.$$

4.5 COMMIX Results

A number of assumptions have been used in the calculation and these assumptions are listed below:

1. No heat loss through the pipe wall of the surge line.
2. No pitch (slope) for horizontal pipe.
3. Calculation started at 17 hr 31 min 10 sec in the transient.

4. Using "best estimate" initial and boundary conditions based on very limited experimental measurements. It is to be noted that these measurements are in graphic plot (see Figs. 2-7), but not in digital form.
5. Approximating L1 pipe as a vertical run.
6. Pipe wall conduction limited to one dimension (radial direction only).

The typical velocity profiles and temperature distributions at ten minutes after started calculation will be presented. Both velocity profiles and temperature distributions at the centerline of the surge line in the vertical planes of L2 and L3 are shown in Figs. 13-20 and Figs. 21-28 respectively. The temperature profiles of the surge line cross sections at the locations of T1, T2, T3, and T4 are presented in Figs. 29-32 respectively, and both inside and outside temperatures of the surge line wall corresponding to the measured locations are also shown in these figures.

4.6 Comparison of COMMIX Results with Measurements

A comparison of the outside surge line wall temperatures calculated by the COMMIX code with the measured data provided by the Westinghouse Electric Corp.¹¹ namely T1, T2, T3, and T4, are shown in Figs. 29-32 respectively. The agreement between the calculated results and the experimental measurements are in reasonable agreement.

5 Discussions and Conclusions

In spite of large uncertainties in constructing the "best estimate" initial and boundary conditions based on limited available measurements, it is gratifying that the agreement between the calculated results obtained from the COMMIX code and the experimental data is reasonably good. In our opinion, the agreement can further be improved if both initial and boundary conditions can be more accurately quantified.

The wall temperatures of surge line were calculated by one dimensional (radial direction only) approximation. The calculated results can be improved if the additional conductions from both circumferential and axial directions are incorporated into the

COMMLX code. We recommend that this additional capability should be implemented into the COMMLX code.

Based on T1 and T4 readings, it appears that there is no flow stratification in both inclined pipe L1 and vertical run L4 after a very short period of time started the calculation as shown in Figs. 2 and 5 respectively. Thus, it seems justifiable to model inclined pipe L1 as a vertical run.

As stated before, the major thrust of this work is to demonstrate the capability of the COMMLX code which can be used to predict when, where, and magnitude of local temperature difference in a flow stratified pipe. Based on the comparison between the calculated results from COMMLX code and the experimental measurements as shown in Figs. 33-36, it seems reasonable to conclude that the COMMLX code has demonstrated its capability for predicting the flow stratification in the surge line. While the COMMLX code has demonstrated its capability to perform flow stratification analysis, it is desirable to have more assessments and validations. In particular, the validation must be carried out to compare the COMMLX results with the well instrumented experiments which are not limited to the temperature measurements, but also include the velocity data.

Based on the calculated velocity profiles and temperature distributions as shown in Figs. 13-20 and Figs. 21-28 respectively ten minutes after start of the calculation, the following important observations may be summarized below.

1. The location of maximum flow stratification or maximum local temperature difference between the top and bottom of the surge line is located at L2 right after the flow passing through the elbow from L1. This location is different from either T1, T2, T3, and T4 locations. From the instrumentation point of view, it is very desirable to have measurements located at or nearby the maximum flow stratification.
2. The calculated velocity profiles after ten minutes during the transient calculation are similar to those shown in Figs. 13-20. The calculated velocity profile in the surge line is very complicated. In a large portion of horizontal pipes L2 and L3, the fluid in both top and bottom of these pipes is flowing in the same direction and in the middle portion the fluid flows in the opposite direction. It is our belief that the flow pattern is

highly sensitive to geometrical arrangement of a surge line as well as operating conditions. Thus, it is very difficult to make a pre-generalization of flow pattern as well as temperature distribution in a stratified pipe.

3. It is interesting to observe that the calculated temperature at the top of the surge line (zero degree) is slightly higher than the temperature at 60° as shown in Fig. 35 at approximately ten minutes in the transient. This is due to the local velocity at the zero degree is higher than the 60° location, thus the corresponding heat transfer coefficient is higher. As we have mentioned before, the pipe wall conduction model used in the COMMLX code is limited to one dimension (radial direction only in this case), the spread of the calculated temperatures between 0° and 90° location of T3 could be larger if the circumferential conduction of the pipe wall is included. Furthermore, the validity of the assumption of no heat loss through the surge line wall needs to be examined for future calculations.

Finally, it is to be noted that the COMMLX code is a general purpose, multidimensional computer program which is not limited to the flow stratification in a surge line. In fact, the COMMLX code can be applied to flow stratification problems occurring in any reactor component such as high pressure injection system, steam generator feedwater ring, etc., under various reactor operating conditions. It has also been used extensively for natural circulation analysis under severe accident conditions. Recently, the NRR/USNRC expressed some concern regarding the thermal stripping problem. It is our belief that, with some modification of the COMMLX code, we will be in a position to tackle the thermal stripping problem as well.

Acknowledgments

The authors gratefully acknowledge the encouragement and support of Drs. Barry Koufer, George Lanik, Jack Rosenthal, and Nelson Su of AEOD, U.S. Nuclear Regulatory Commission. Stimulating discussions with our coworkers Drs. M. Bottoni, T. H. Chien and H. M. Domanus and the excellent typing of S. Moll are also acknowledged.

References

1. Su, Nelson T. *Special Study Report Review of Thermal Stratification Operating Experience*, AEOD/S902 (March 1990).
2. Domanus, H. M. and W. T. Sha, *Analysis of Natural Convection Phenomena in a 3-Loop PWR During a TMLB' Transient using the COMMIX Code*, NUREG/CR-5070, ANL-87-54 (December 1987).
3. Sha, W. T., et al., *COMMIX-1: A Computer Program for Three-Dimensional, Transient, Single-Phase Thermal Hydraulic Analysis*, NUREG/CR-0483, ANL-77-96 (September 1978).
4. Sha, W. T., et al., *COMMIX-1B: A Three-Dimensional Transient Single-Phase Computer Program for Thermal Hydraulic Analysis of Single and Multicomponent Systems*, NUREG/CR-4348, ANL-85-42 (September 1985).
5. Domanus, H. M. et al., *COMMIX-1C: A Three-Dimensional Transient Single-Phase Computer Program for Thermal Hydraulic Analysis of Single- and Multicomponent Engineering Systems*, NUREG/CR-5649, ANL-90/33 (September 1990).
6. Sha, W. T., B. T. Chao, and S. L. Soo, *Conservation Equations for Finite Control Volume Containing Single Phase Fluid with Fixed, Dispersed Heat Generating (or Absorbing) Solids*, NUREG/CR-0945 ANL-CT-79-42 (July 1979).
7. Harlow, F. H., and A. A. Amsden, *A Numerical Fluid Dynamics Calculation Method for All Flow Speeds*, J. Computational Phys., **8**, p. 197 (1971).
8. Harlow, F. H., and A. A. Amsden, *Numerical Calculation of Multiphase Fluid Flow*, J. Computational Phys., **17**, pp. 19-52 (1975).
9. F. H. Harlow and A. A. Amsden, *Flow of Interpenetrating Material Phases*, J. Computational Phys., **18**, pp. 440-464 (1975).

10. Patankar, S. V., *Numerical Heat Transfer and Fluid Flow*, in Numerical Heat Transfer, Vol. 2, New York:McGraw-Hill (1979).
11. FAX from Bill Coslow of Westinghouse Power Systems Division to W. T. Sha of Argonne National Laboratory, dated September 25, 1990.

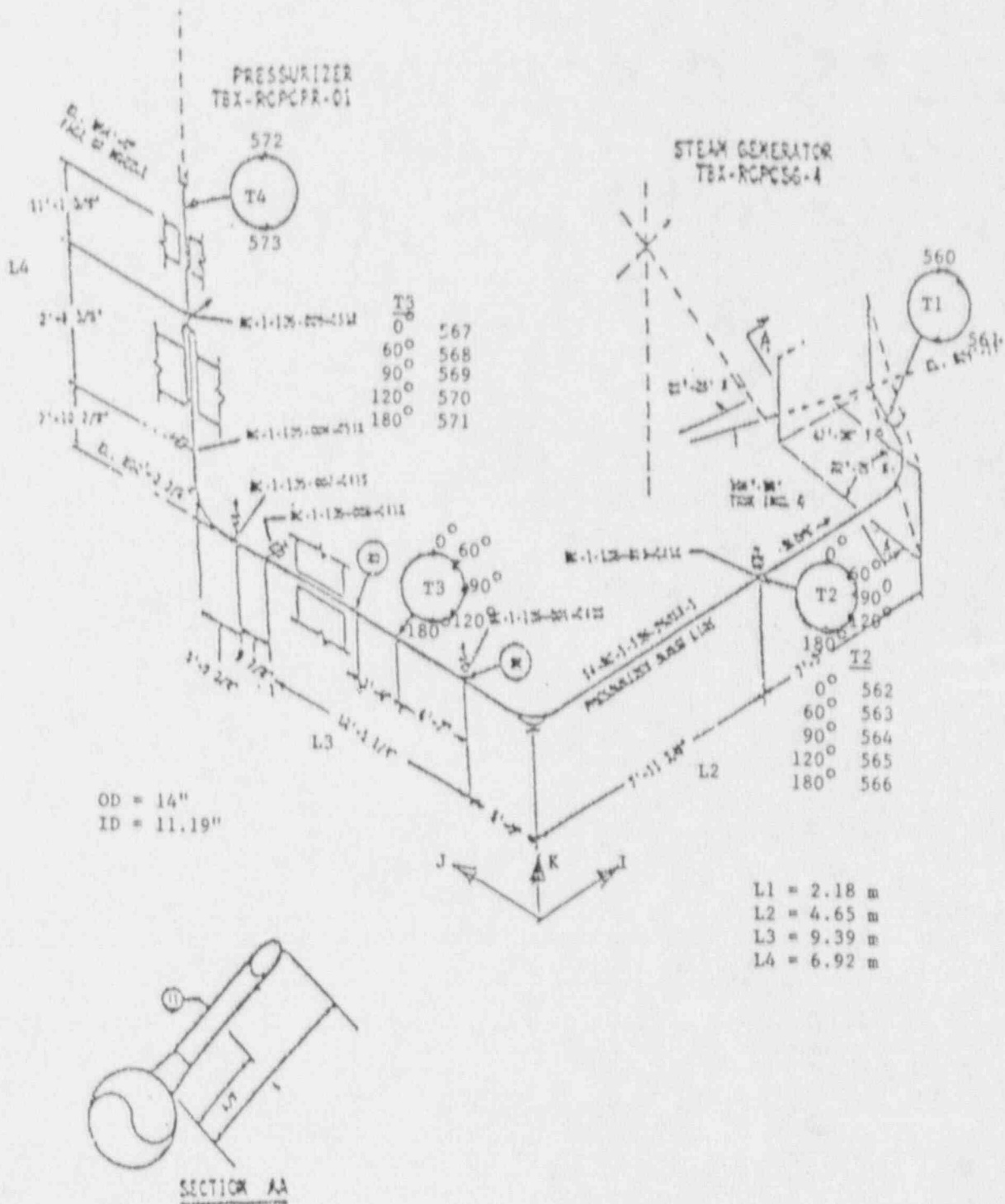


Fig. 1. Pressurizer Surge Line Layout and Monitoring Locations

COMANCHE PEAK STEAM ELECTRIC STATION - UNIT 1
STRATIFICATION AND THERMAL CYCLING

STRATIFY
Revision 0
3 Mar 1990

CH-560				CH-561			
PZR	SGL	PT	TEMP	PZR	SGL	PT	TEMP
Minimum	-	151.835	DEGF	Minimum	-	151.190	DEGF
Maximum	-	350.549	DEGF	Maximum	-	200.737	DEGF
Average	-	193.062	DEGF	Average	-	185.979	DEGF
SD	-	10.595	DEGF	SD	-	12.012	DEGF

Top Curve

Bottom Curve

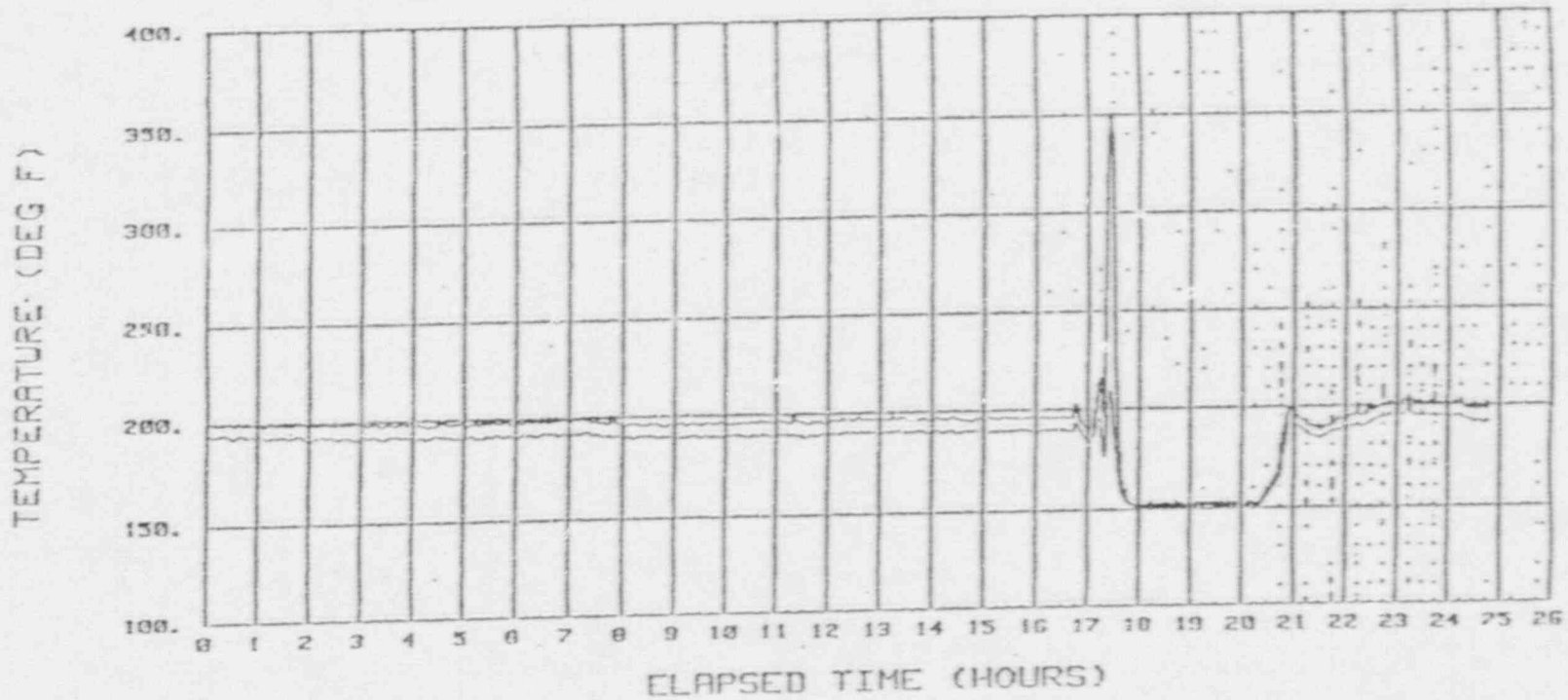


Fig. 2. TI Readings

DRAFT

COMANCHE PEAK STEAM ELECTRIC STATION -- UNIT 1
 STRATIFICATION AND THERMAL CYCLING

CH-562			CH-563			CH-564		
PZR	SGL	TEMP	PZR	SGL	TEMP	PZR	SGL	TEMP
Minimum	253.384	DEGF	Minimum	239.283	DEGF	Minimum	216.135	DEGF
Maximum	408.187	DEGF	Maximum	409.330	DEGF	Maximum	410.073	DEGF
Average	393.373	DEGF	Average	390.939	DEGF	Average	386.993	DEGF
SD	36.158	DEGF	SD	44.686	DEGF	SD	37.365	DEGF
CH-565			CH-566					
PZR	SGL	TEMP	PZR	SGL	TEMP			
Minimum	175.474	DEGF	Minimum	150.831	DEGF			
Maximum	407.420	DEGF	Maximum	382.923	DEGF			
Average	379.828	DEGF	Average	351.784	DEGF			
SD	68.469	DEGF	SD	72.373	DEGF			

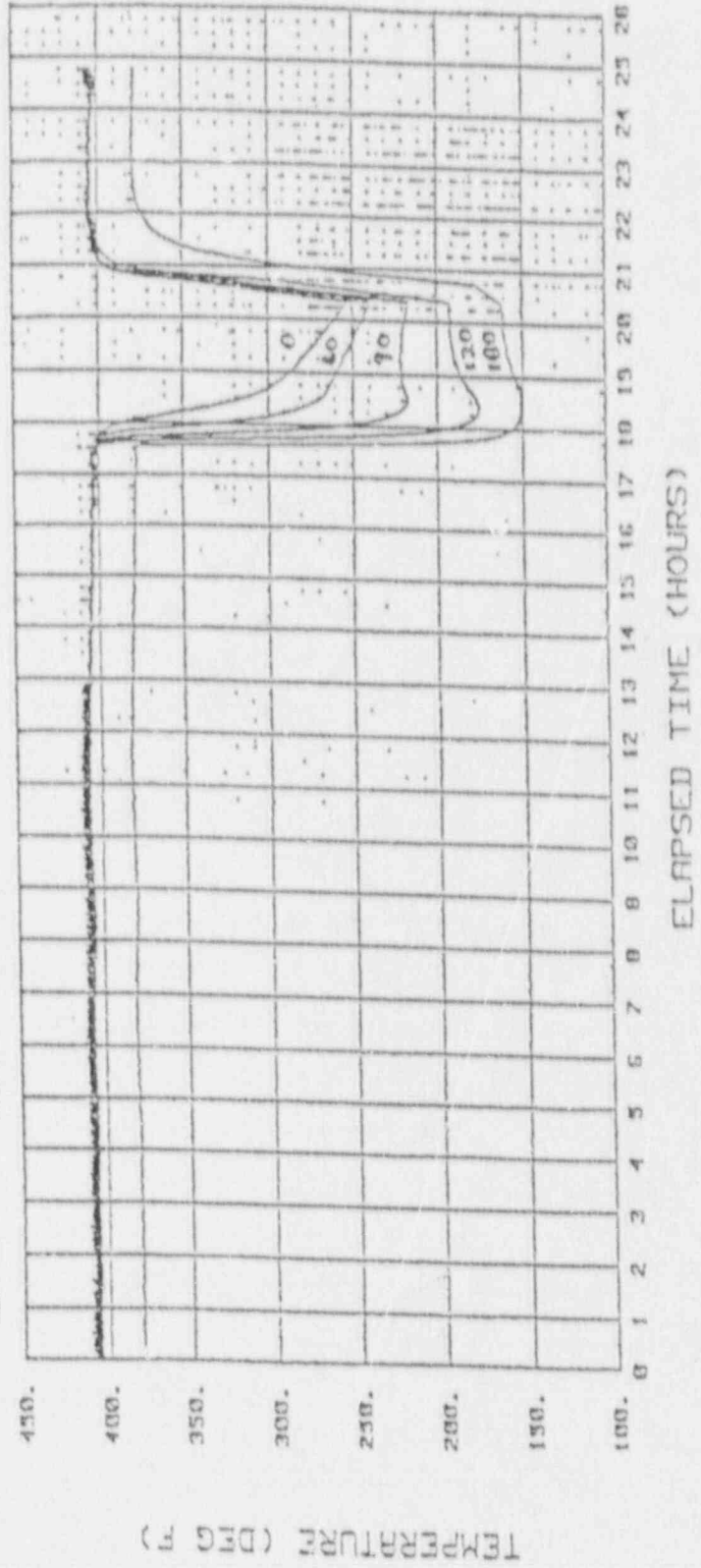


Fig. 3. T2 Readings

COMANCHE PEAK STEAM ELECTRIC STATION - UNIT 1
STRATIFICATION AND THERMAL CYCLING

CH-567		CH-569		CH-569	
PZR	SGL	PT	PT	PZR	SGL
Minimum	272.452	Minimum	240.904	Minimum	221.359
Maximum	438.897	Maximum	427.787	Maximum	423.189
Average	415.852	Average	409.748	Average	393.561
SD	34.997	SD	45.318	SD	57.018

CH-570		CH-571	
PZR	SGL	PZR	SGL
Minimum	189.126	Minimum	158.454
Maximum	409.338	Maximum	365.523
Average	382.533	Average	338.841
SD	65.346	SD	65.384

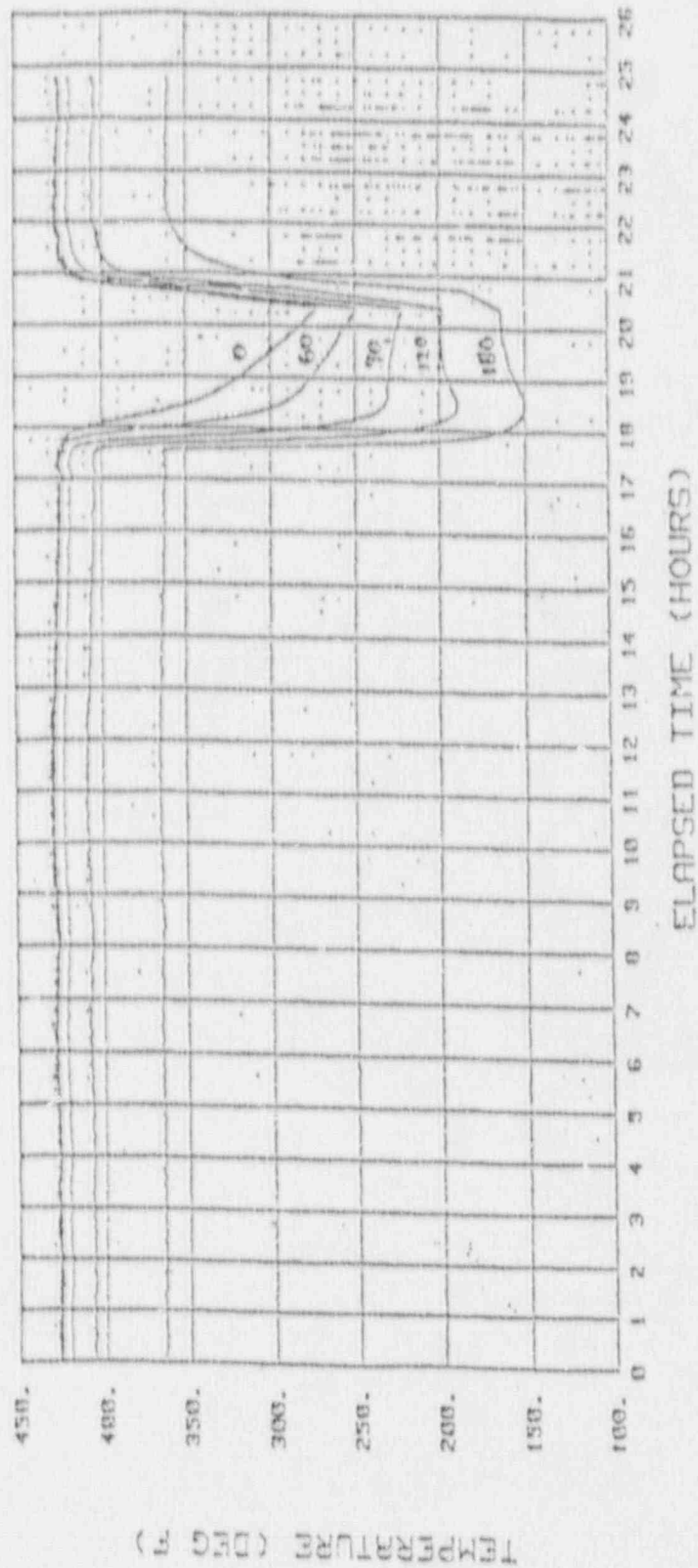


Fig. 4. T3 Readings

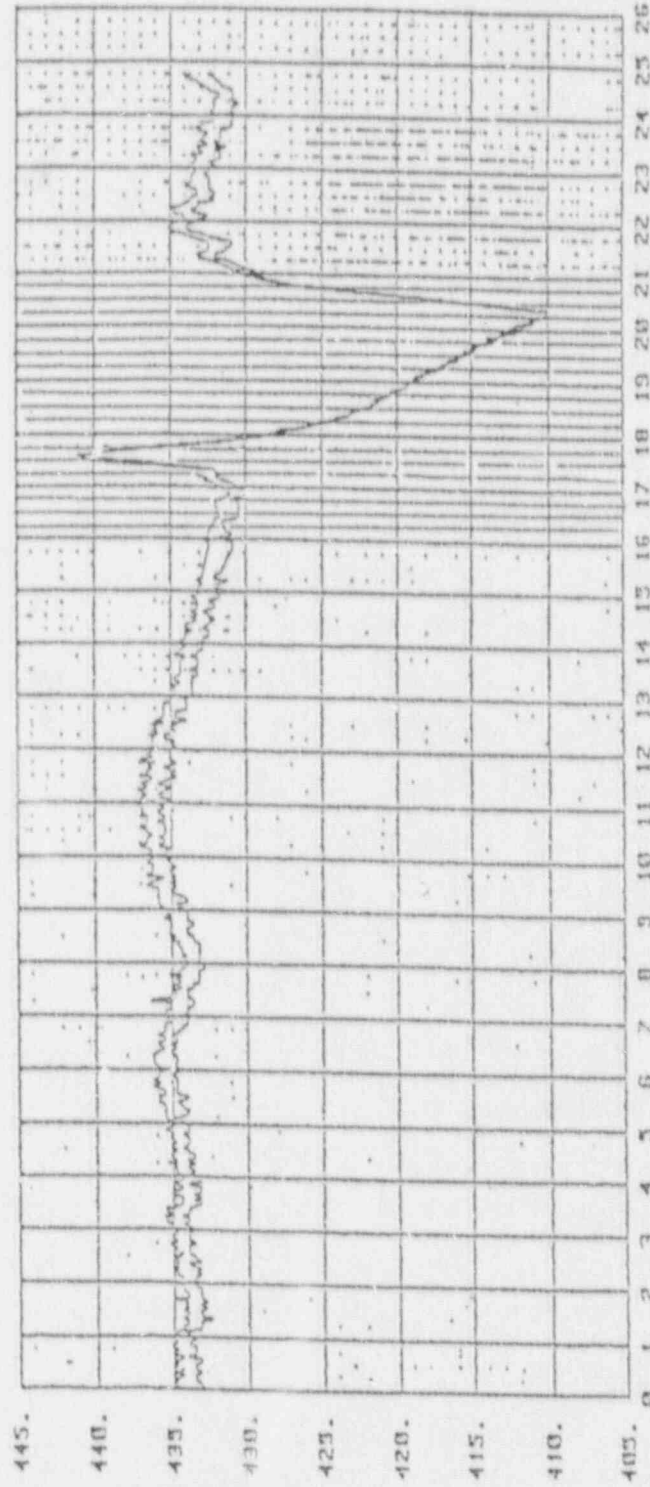
COMANCHE PEAK STEAM ELECTRIC STATION - UNIT 1
 STRATIFICATION AND THERMAL CYCLING

STRATIFY
 Revision B
 3 Mar 1990

CH-572		CH-573	
PZR	SGL	PZR	SGL
PT	PT	PT	PT
00T-4-000	00T-4-100	00T-4-100	TEMP
Minimum - 410.106 DEGF	Minimum - 410.106 DEGF	Maximum - 440.891 DEGF	
Maximum - 439.793 DEGF	Maximum - 431.817 DEGF	Average - 432.860 DEGF	
Average - 431.817 DEGF	SD - 5.217 DEGF	SD - 5.496 DEGF	

Bottom Curve

Top Curve



ELAPSED TIME (HOURS)

Fig. 5. T4 Readings

TEMPERATURE (DEG F)

COMANCHE PEAK STEAM ELECTRIC STATION - UNIT 1
STRATIFICATION AND THERMAL CYCLING

STRATIFY
Revision 0
9 Mar 1990

CH-054		CH-055		CH-056		CH-057	
RCS LP1 HL TEMP (NR)		RCS LP2 HL TEMP (NR)		RCS LP3 HL TEMP (NR)		RCS LP4 HL TEMP (NR)	
Minimum	- 154.000 DEGF	Minimum	- 154.175 DEGF	Minimum	- 154.000 DEGF	Minimum	- 152.600 DEGF
Maximum	- 162.925 DEGF	Maximum	- 163.100 DEGF	Maximum	- 160.025 DEGF	Maximum	- 163.625 DEGF
Average	- 157.502 DEGF	Average	- 157.909 DEGF	Average	- 157.196 DEGF	Average	- 158.214 DEGF
SD	- 2.400 DEGF	SD	- 2.332 DEGF	SD	- 1.600 DEGF	SD	- 2.760 DEGF

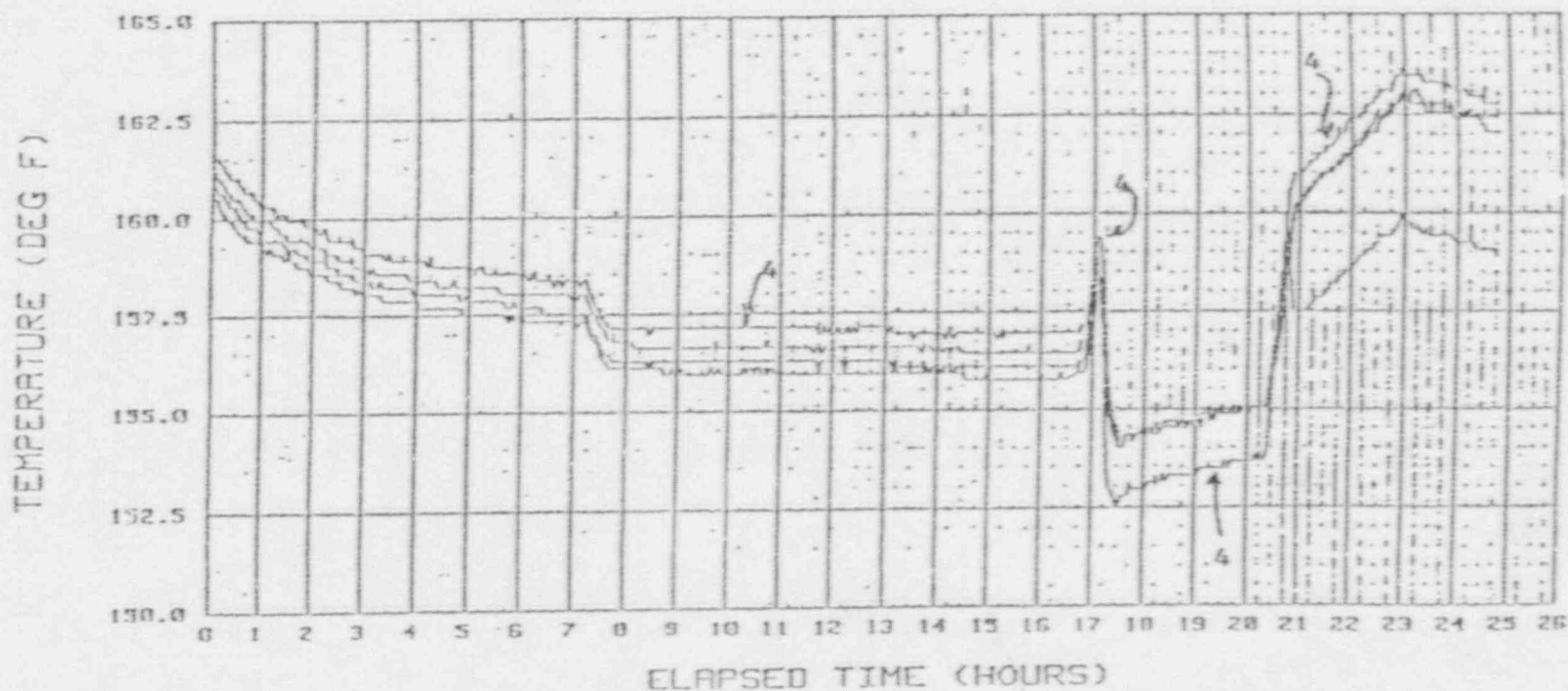
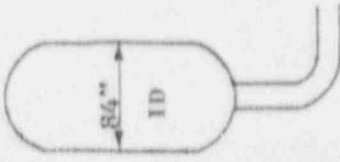


Fig. 6. Hot Leg Temperature Reading

DRAFT

COMANCHE PEAK STEAM ELECTRIC STATION - UNIT 1
 STRATIFICATION AND THERMAL CYCLING

STIMIFY
 Revision 0
 9 Mar 1990



Vol
 = 1800 ft³

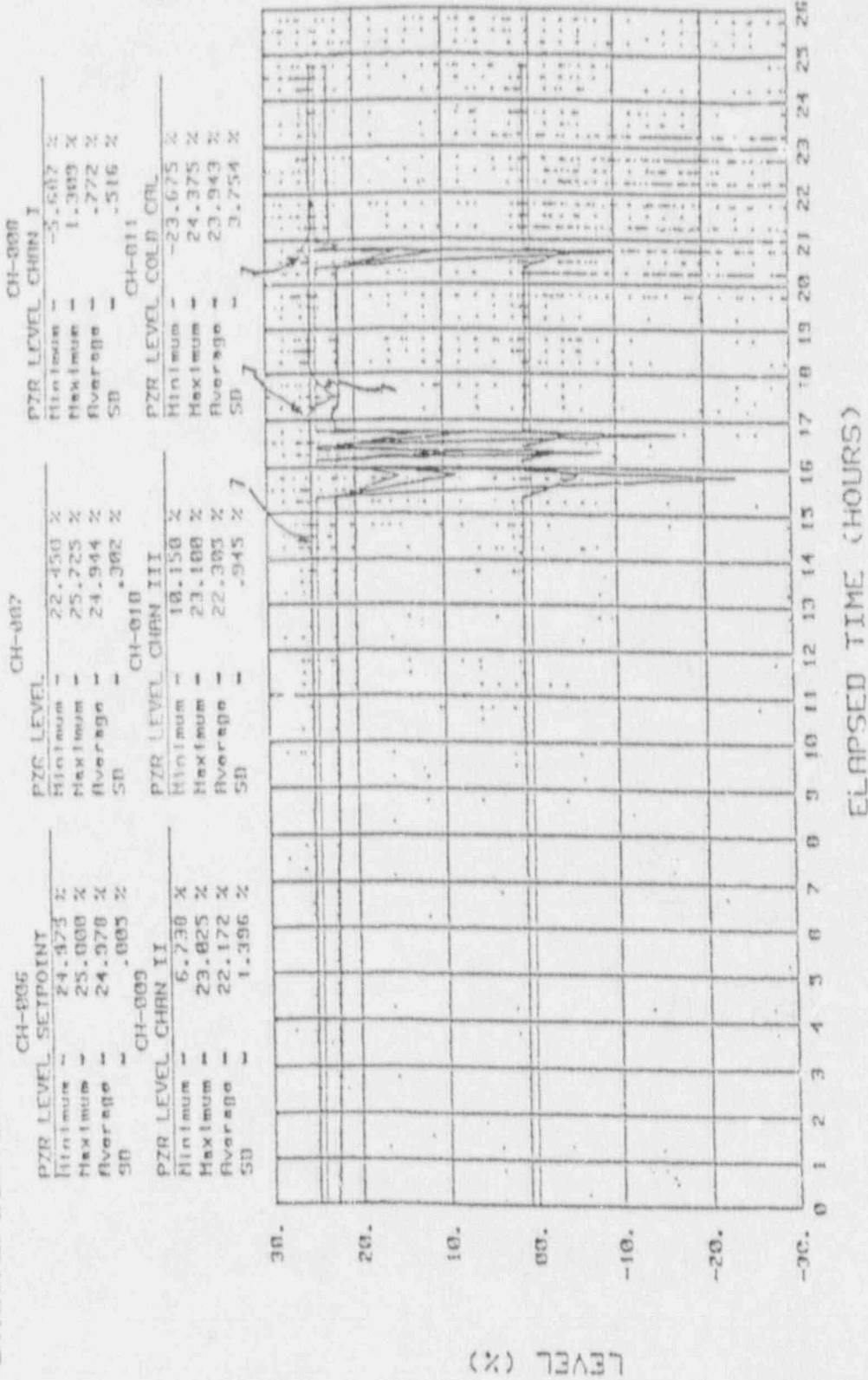


Fig. 7. Pressurizer Water Level Reading

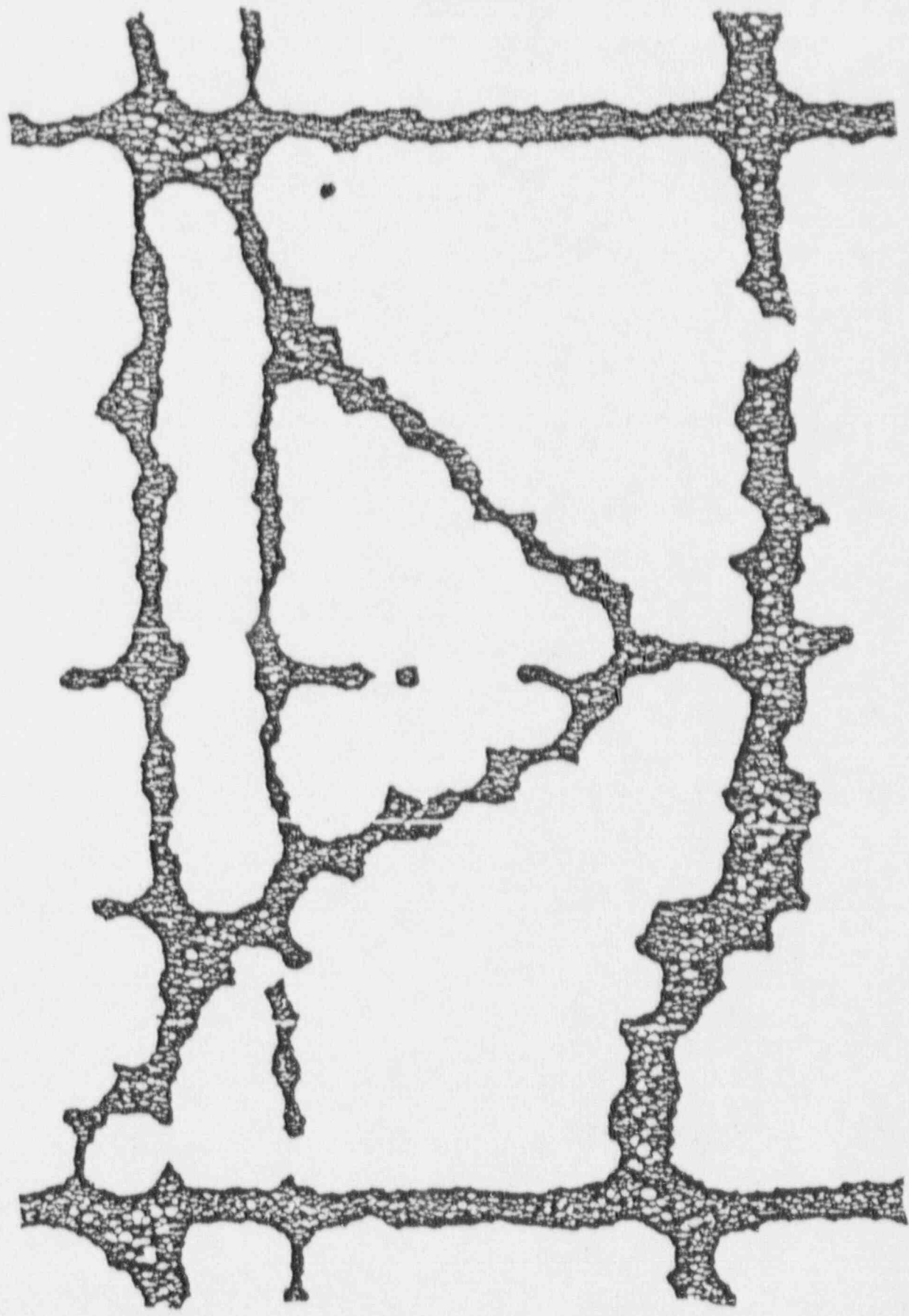


Fig. 7a. Enlarged View of a Portion of Fig. 7

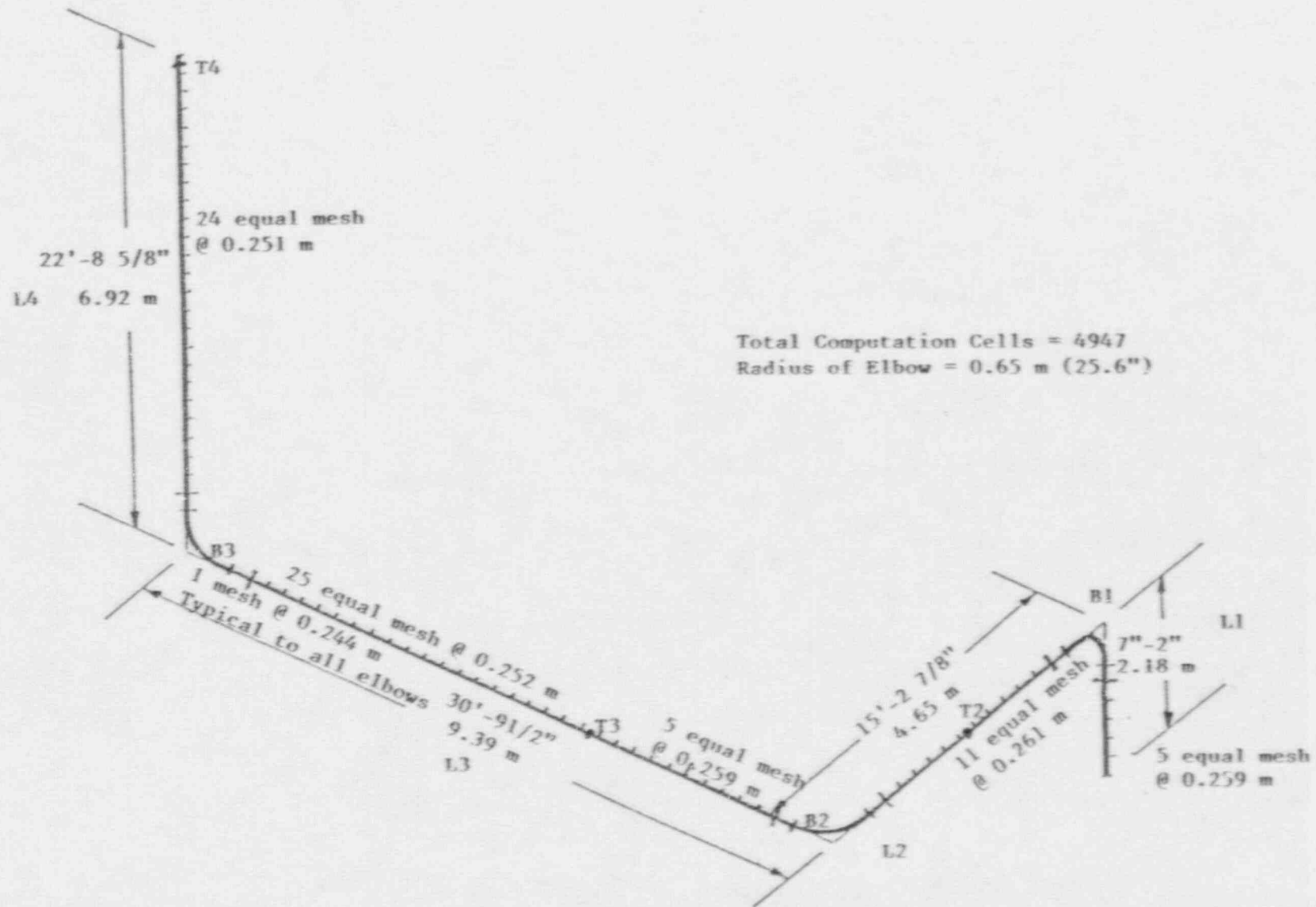


Fig. 8. Surge Line Layout Used in COMMIX Code

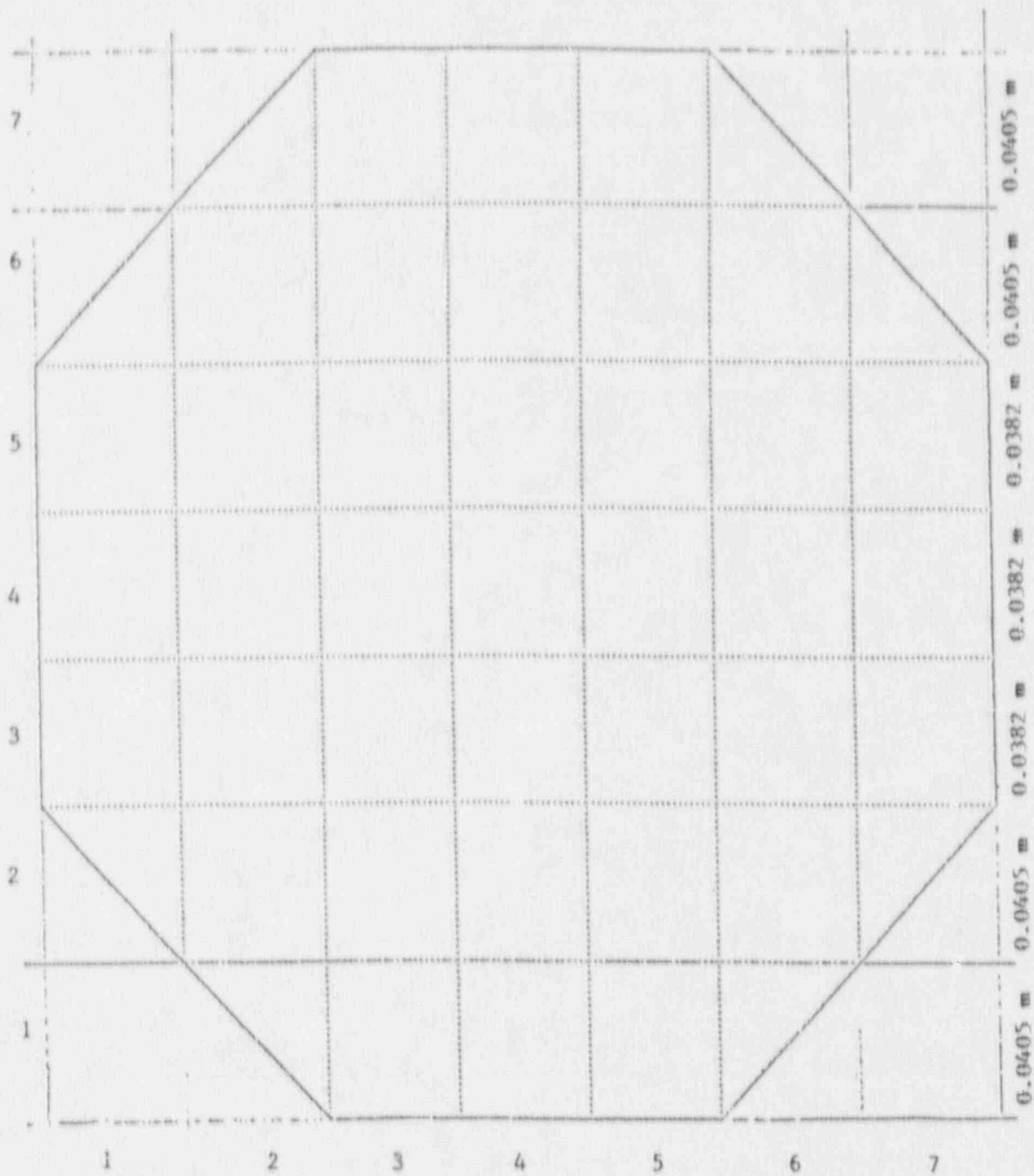


Fig. 9. Typical Cross Section of Surge Line

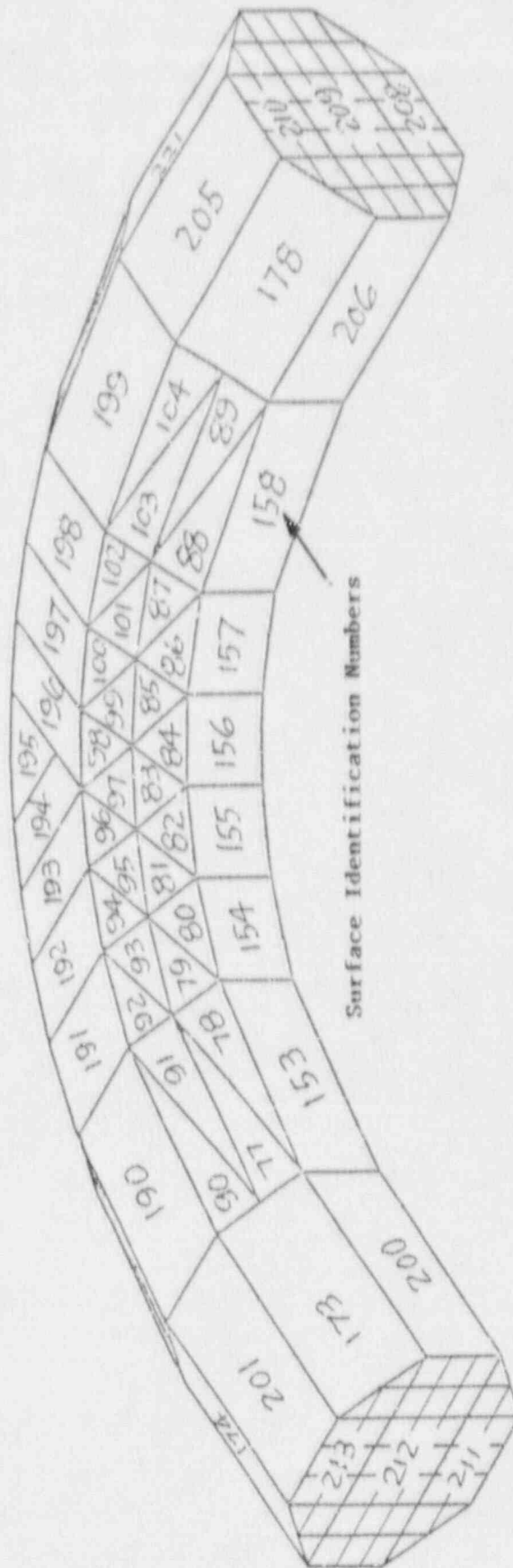


Fig. 10. Typical Elbow

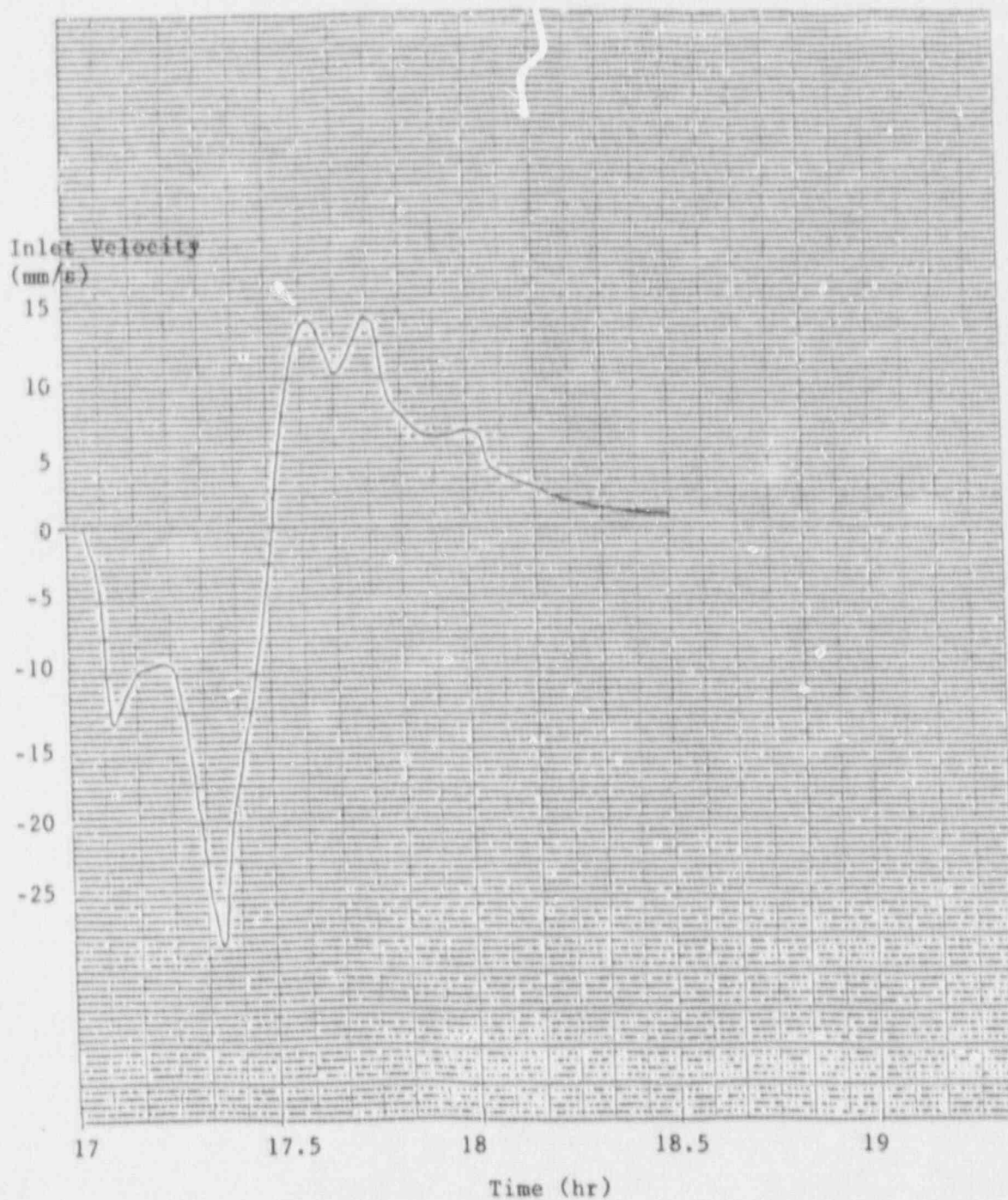


Fig. 11. Inlet Velocity of the Surge Line

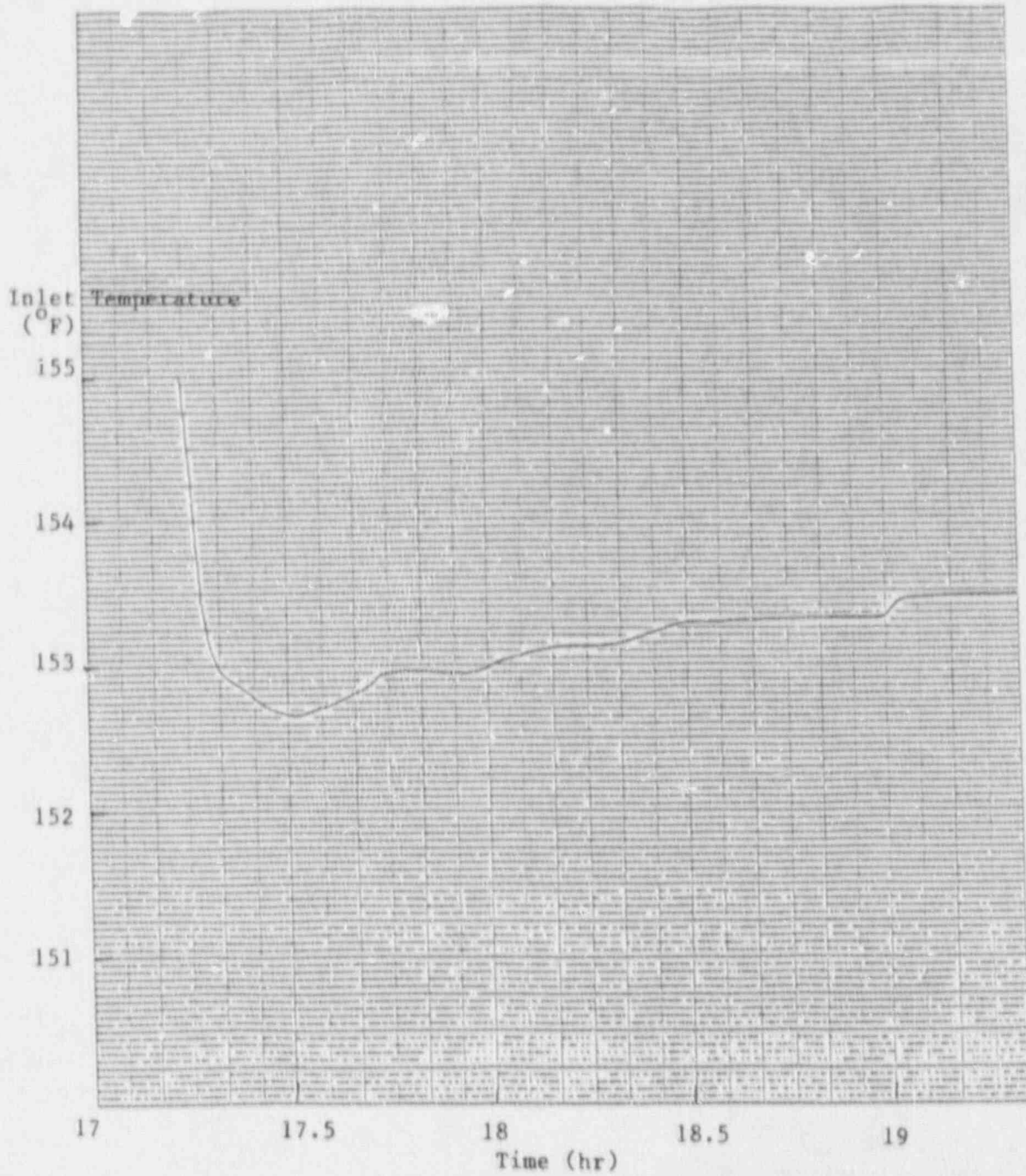


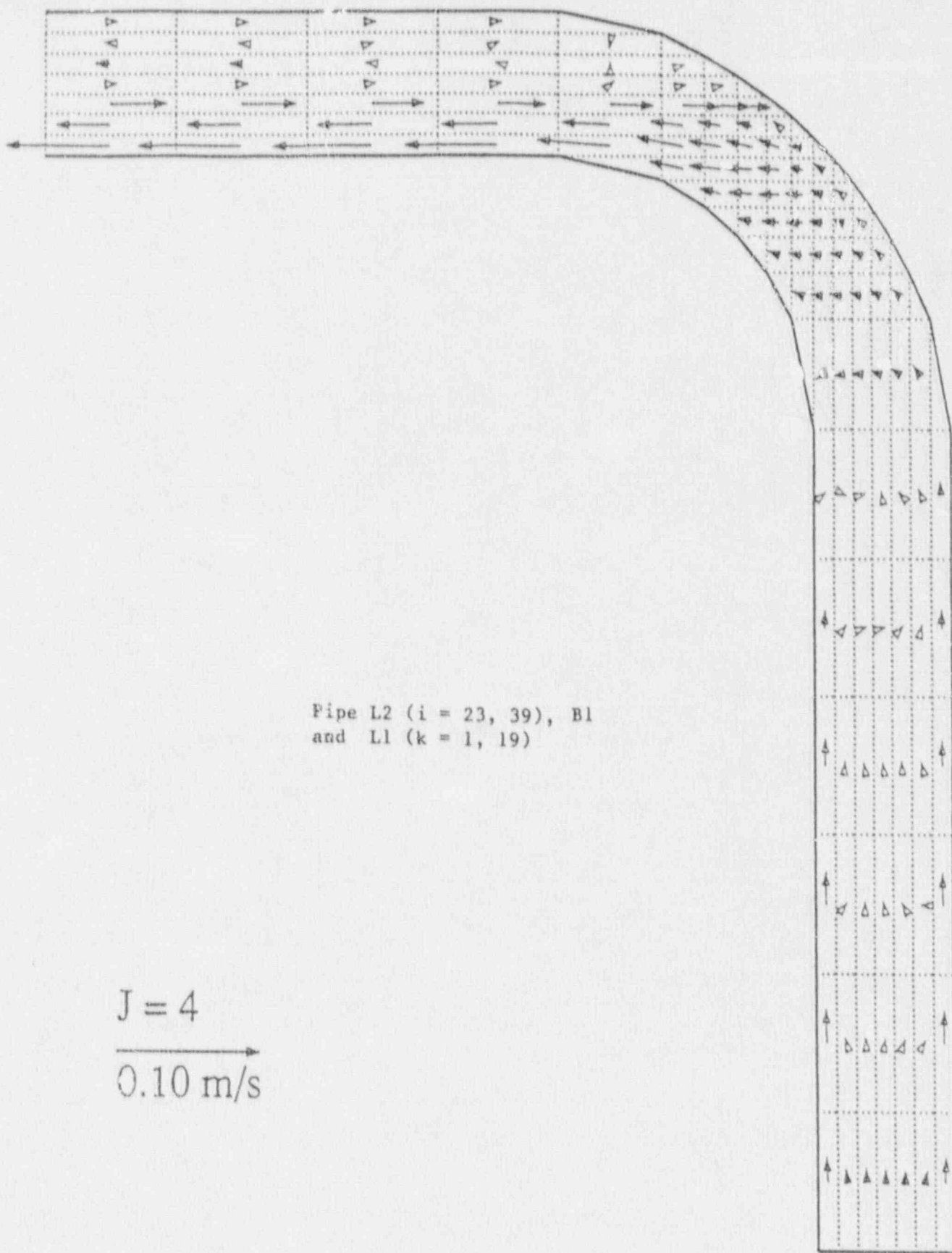
Fig. 12. Inlet Temperature of the Surge Line

Table 1. Pressurizer Water Level vs Volume

INSIDE DIAMETER: 64.000 INCHES TOTAL INSIDE LENGTH OF TANK: 578.500 INCHES
 HEIGHT OF TANK CYLINDER: 530.000 INCHES DEPTH OF ELLIPTICAL HEADS: 30.000 INCHES
 LEVEL INDICATION BEGINS AT 39.000 INCHES LEVEL INDICATION ENDS AT 561.500 INCHES

LIQUID HEIGHT (INCHES)	VOLUME (GALLONS)	LEVEL IND. (%)	LIQUID HEIGHT (INCHES)	VOLUME (GALLONS)	LEVEL IND. (%)	LIQUID HEIGHT (INCHES)	VOLUME (GALLONS)	LEVEL IND. (%)
39.00	604.5	0.00	45.00	809.7	1.00	50.00	934.8	2.00
55.40	1060.0	3.00	60.67	1185.2	4.00	65.00	1310.3	5.00
71.80	1425.5	6.00	76.32	1560.6	7.00	80.54	1605.8	8.00
88.20	1810.9	9.00	91.97	1936.1	10.00	97.19	2061.3	11.00
104.60	2166.4	12.00	107.62	2311.6	13.00	112.84	2436.7	14.00
118.86	2561.9	15.00	123.27	2687.0	16.00	128.47	2812.2	17.00
133.71	2937.4	18.00	138.92	3162.5	19.00	144.14	3187.7	20.00
149.36	3312.8	21.00	154.57	3438.0	22.00	159.79	3563.1	23.00
165.01	3688.3	24.00	170.23	3813.5	25.00	175.44	3938.6	26.00
180.66	4063.8	27.00	185.88	4189.0	28.00	191.09	4314.1	29.00
196.31	4439.3	30.00	201.53	4564.4	31.00	206.74	4689.6	32.00
211.96	4814.7	33.00	217.18	4939.9	34.00	222.40	5065.1	35.00
227.61	5190.2	36.00	232.83	5315.4	37.00	238.05	5440.5	38.00
243.26	5565.7	39.00	248.48	5690.8	40.00	253.70	5816.0	41.00
258.91	5941.1	42.00	264.13	6066.3	43.00	269.35	6191.5	44.00
274.57	6316.6	45.00	279.78	6441.8	46.00	285.00	6566.9	47.00
291.22	6692.1	48.00	295.43	6817.2	49.00	300.65	6942.4	50.00
306.87	7167.6	51.00	311.08	7192.7	52.00	316.30	7317.9	53.00
321.52	7643.0	54.00	326.74	7568.2	55.00	331.95	7693.4	56.00
337.17	8118.5	57.00	342.39	7943.7	58.00	347.60	8068.9	59.00
352.82	8594.0	60.00	358.04	8319.1	61.00	363.25	8444.3	62.00
368.47	9069.5	63.00	373.69	8694.6	64.00	378.90	8819.8	65.00
384.12	9544.9	66.00	389.34	9070.1	67.00	394.55	9195.2	66.00
399.77	10020.4	69.00	404.99	9445.6	70.00	410.20	9570.7	71.00
415.42	10495.9	72.00	420.64	9821.1	73.00	425.85	9946.2	74.00
431.07	10971.3	75.00	436.29	10196.5	76.00	441.50	10321.7	77.00
446.73	11446.8	78.00	451.94	10572.0	79.00	457.15	10697.1	80.00
462.38	11922.3	81.00	467.59	10947.4	82.00	472.80	11072.6	83.00
478.03	12397.8	84.00	483.25	11322.9	85.00	488.45	11448.1	86.00
493.68	12873.2	87.00	498.90	11698.4	88.00	504.10	11823.6	89.00
509.33	13348.7	90.00	514.55	12073.9	91.00	519.75	12199.1	92.00
524.98	13824.2	93.00	530.20	12449.3	94.00	535.40	12574.5	95.00
540.63	14299.7	96.00	545.85	12824.8	97.00	551.05	12950.0	98.00
556.28	14775.1	99.00	561.50	13200.3	100.00			

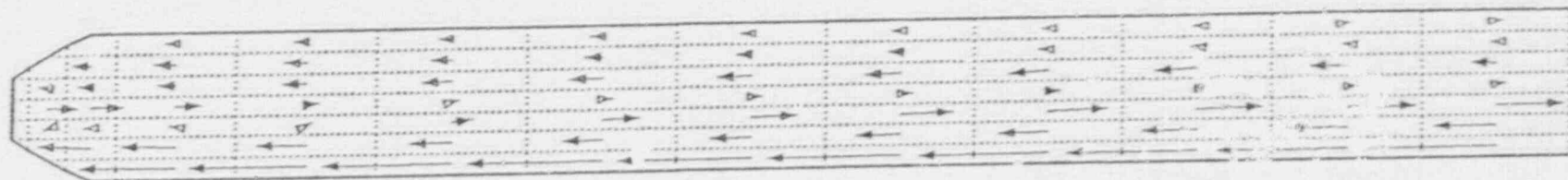
TITLE: PRESSURIZER PREPARED BY: *AW Smith 2/21/90*
 SOURCE: TECHNICAL SUPPORT REVIEWED BY: *J. S. Huley 2/2/90*



Pipe L2 (i = 23, 39), B1
and L1 (k = 1, 19)

$J = 4$
→
0.10 m/s

Fig. 13. Velocity Profile at 10 min. in the Transient



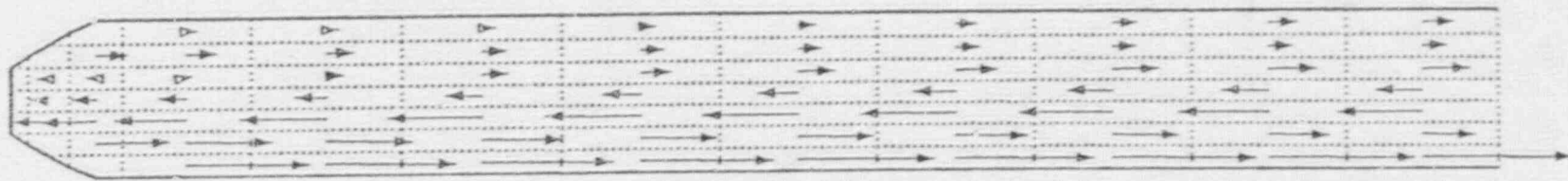
$J = 4$

$\overrightarrow{0.10 \text{ m/s}}$

Pipe L2 ($i = 10, 22$)

Fig. 14. Velocity Profile at 10 Min. in Transient

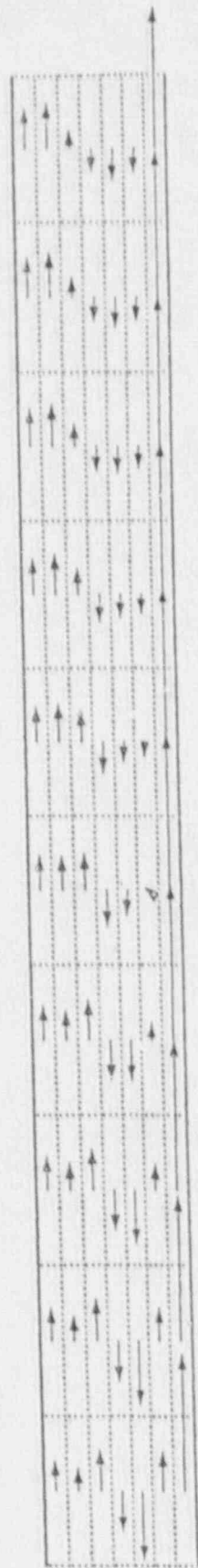
DRAFT



Pipe L3 (j = 10, 21) and B2

$I = 4$
→
0.10 m/s

Fig. 15. Velocity Profile at 10 Min. in Transient

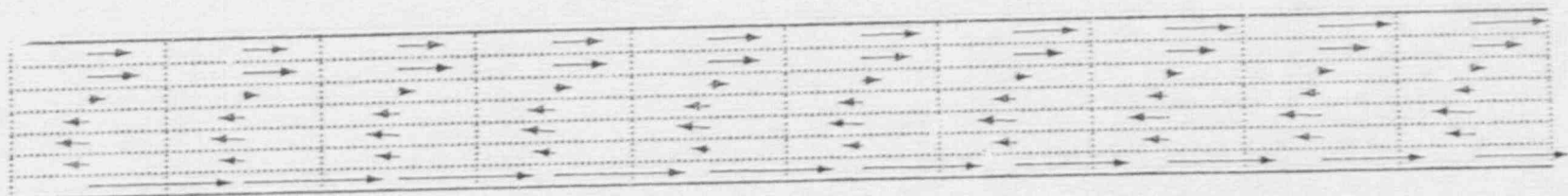


$I = 4$

$\overline{0.10 \text{ m/s}}$

Pipe L3 ($j = 22, 31$)

Fig. 16. Velocity Profile at 10 Min in Transient

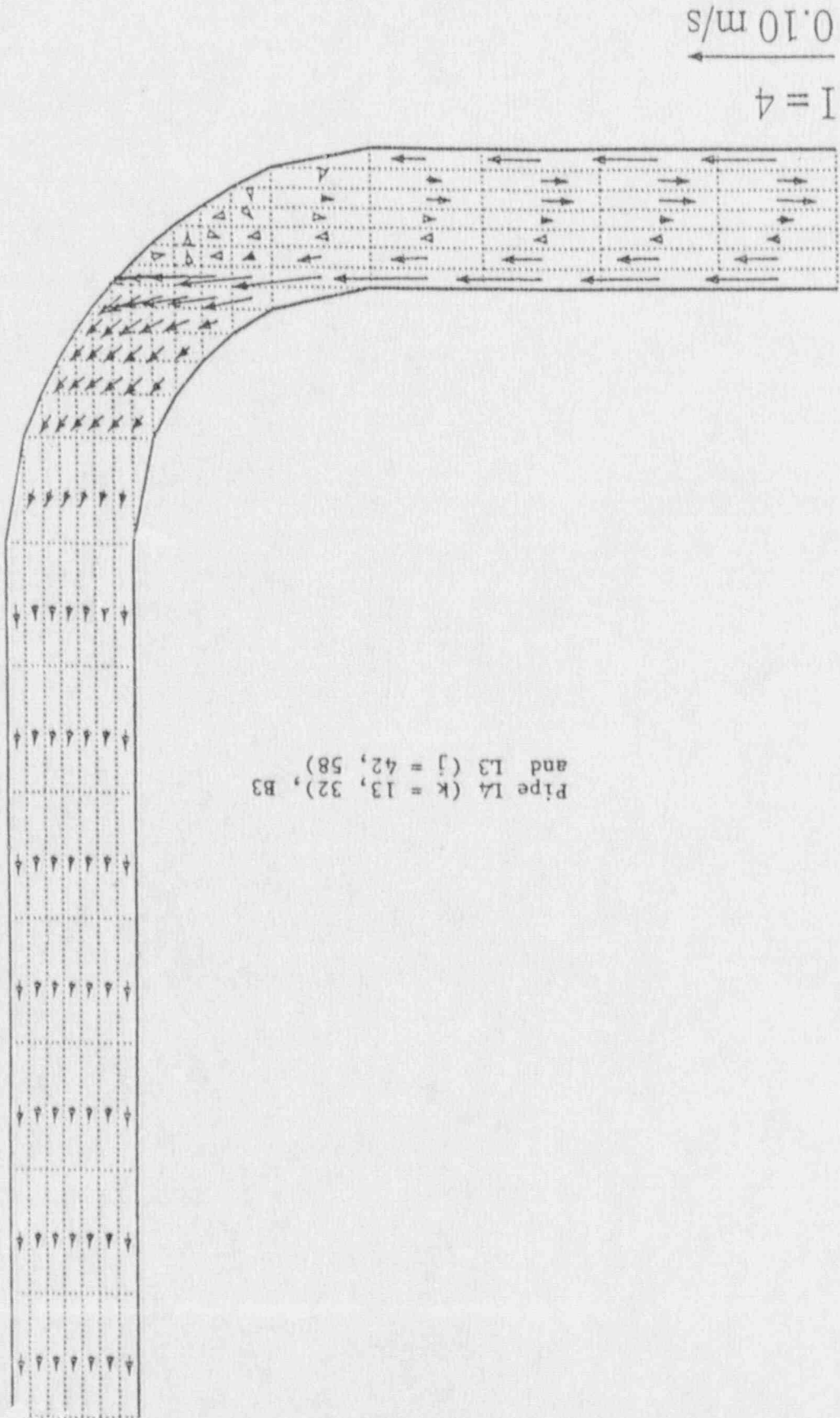


$I = 4$
→
0.10 m/s

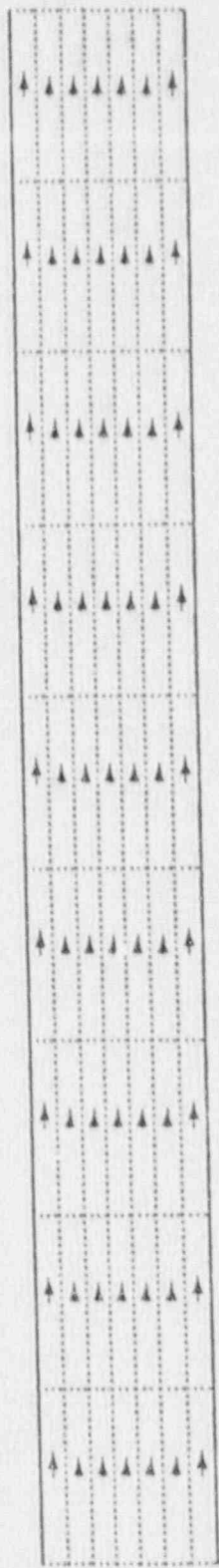
Pipe L3 (j = 32, 41)

Fig. 17. Velocity Profile at 10 Min. in Transient

Fig. 18. Velocity Profile at 10 Min. in Transient



DRAFT



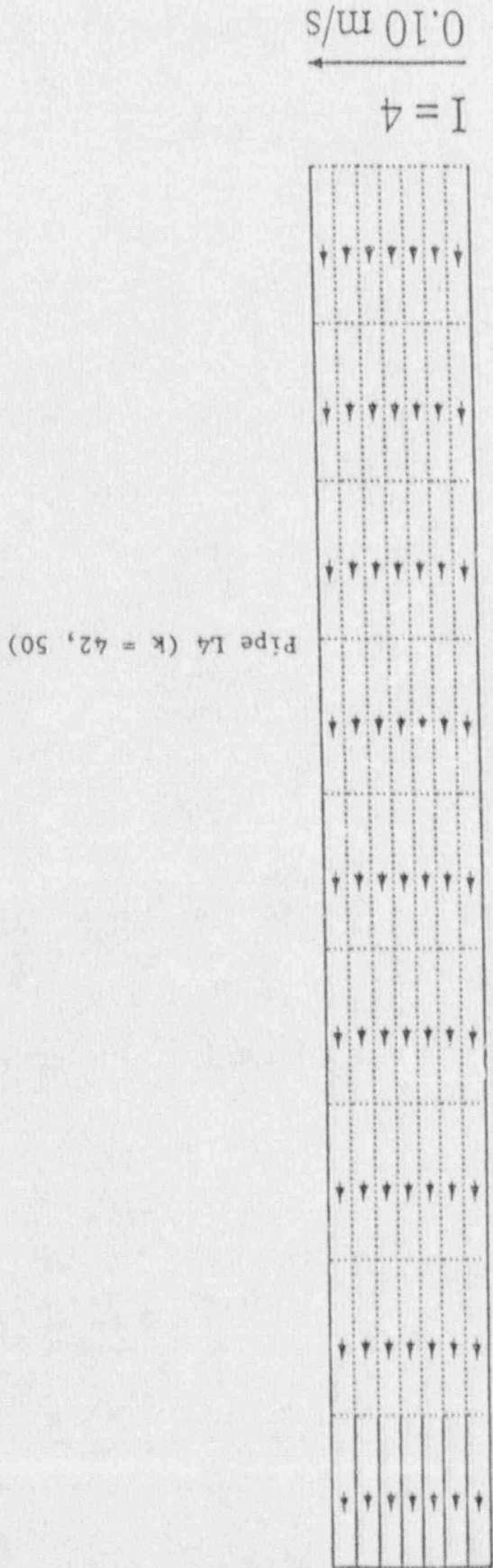
Pipe L4 ($k = 33, 41$)

$$I = 4$$

→
0.10 m/s

Fig. 19. Velocity Profile at 10 Min. in Transient

FIG. 20. Velocity Profile at 10 Min. in Transient



DRAFT

	207	201	202	201	199	198	197	196	196	195	195	194
180°	183	184	182	183	184	185	187	188	189	189	190	189
175°	175	174	174	173	172	171	169	168	167	166	165	165
144°	145	145	145	146	148	149	150	152	153	154	156	157
140°	138	132	137	136	135	135	135	135	136	135	135	135
90°	98	98	100	103	104	104	103	101	99	98	97	96
8°	85	86	85	85	85	85	84	83	82	80	78	77

$J = 4$

Pipe L2 (i = 10, 22)

Fig. 22. Temperature Distributions at 10 Min. in Transient

	207	202	202	202	201	200	199	199	198	198	198
182	187	183	183	184	185	185	186	186	187	187	186
170	170	169	169	168	168	168	168	168	168	168	169
148	149	150	151	151	151	151	151	151	150	149	148
138	137	137	137	136	136	136	135	135	135	135	135
117	117	112	112	113	113	113	114	115	116	118	119
97	97	95	97	99	101	101	102	103	105	106	107

$I = 4$

Pipe L3 (j = 10, 21) & B2

Fig. 23. Temperature Distributions at 10 Min. in Transient

DRAFT

198	199	199	200	200	201	200	200	200	200
186	186	185	185	184	184	184	185	185	185
169	170	171	171	172	171	170	170	169	169
147	147	146	144	143	144	145	145	146	146
134	134	133	133	132	132	132	132	131	130
121	123	126	128	131	131	131	130	130	129
108	109	110	110	111	111	111	112	112	112

$I = 4$

Pipe L3 (j = 22, 31)

Fig. 24. Temperature Distributions at 10 Min. in Transient

DRAFT

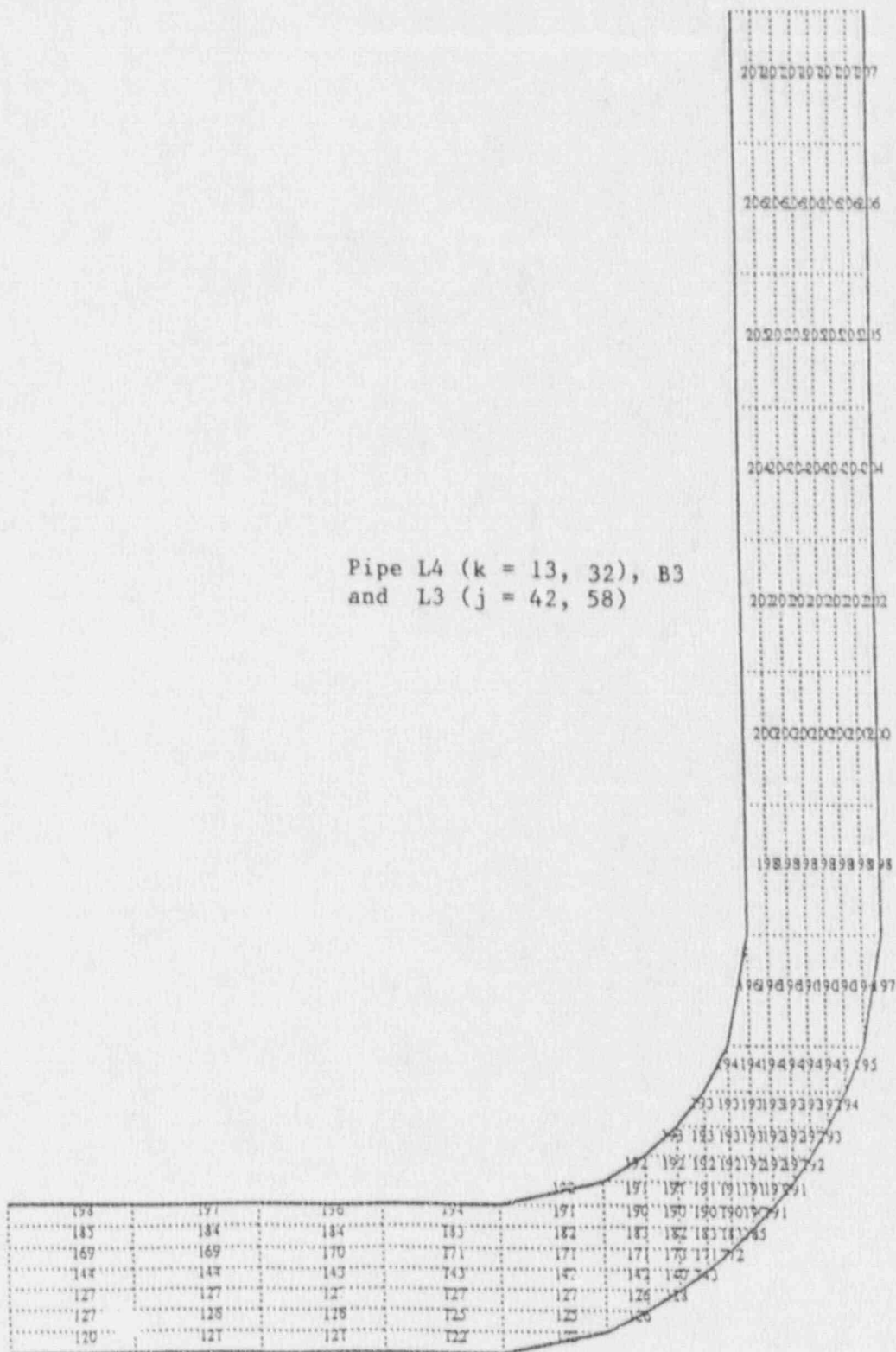
201	201	201	201	200	199	199	199	198	198
185	185	185	186	186	186	186	185	185	185
169	169	168	168	168	169	169	169	169	169
146	146	146	146	146	145	145	145	145	145
130	130	129	129	129	129	129	128	128	128
129	128	128	128	128	128	128	128	127	127
113	113	114	115	116	116	117	118	118	119

I = 4

Pipe L3 (j = 32, 41)

Fig. 25. Temperature Distributions at 10 Min. in Transient

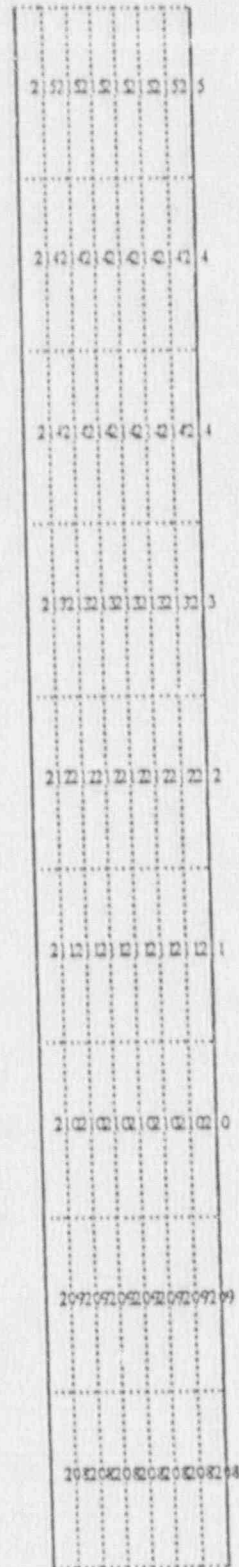
Pipe L4 (k = 13, 32), B3
and L3 (j = 42, 58)



I = 4

Fig. 26. Temperature Distributions at 10 Min. in Transient

Pipe 14 (k = 33, 41)



$$I = 4$$

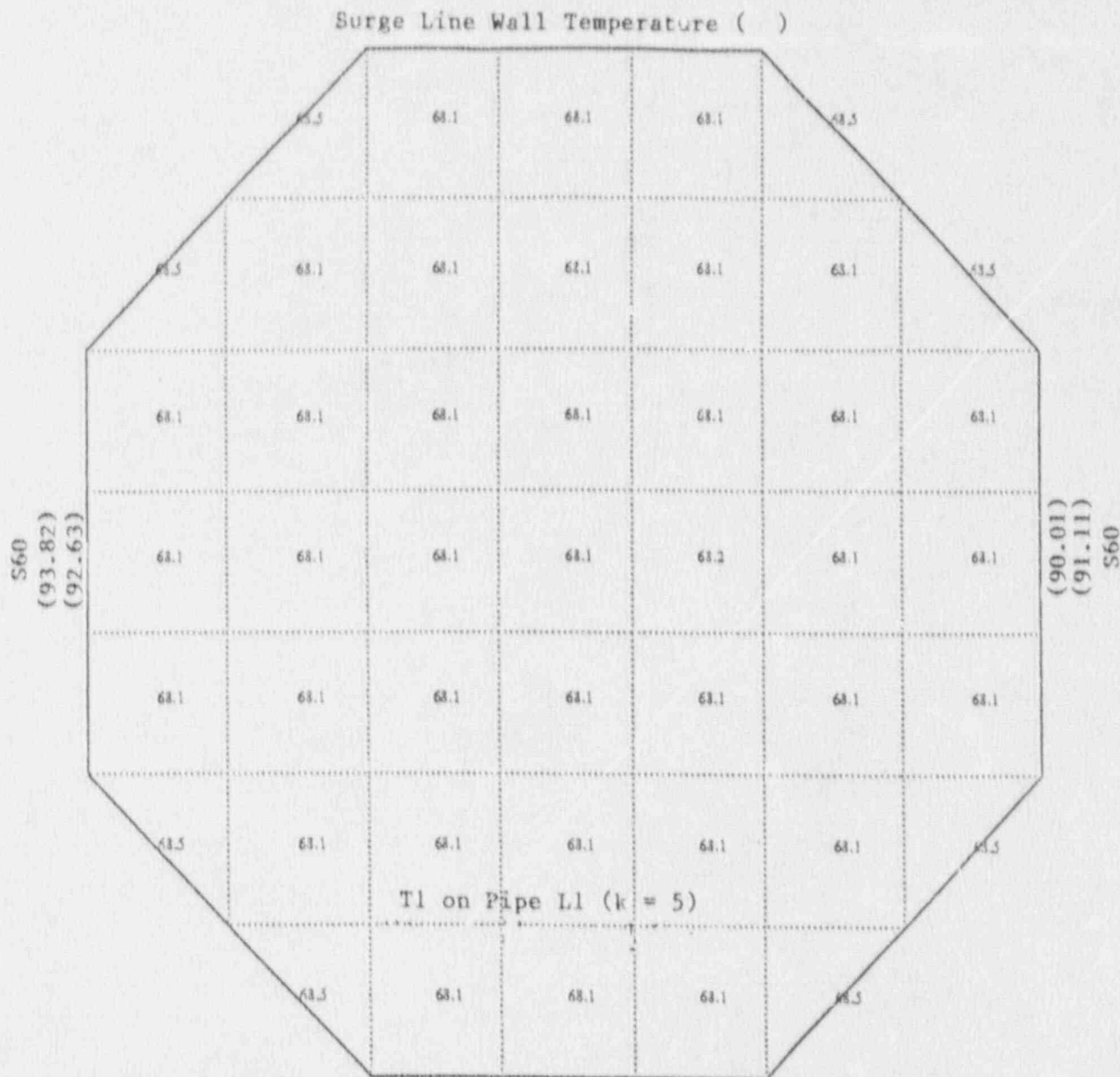
Fig. 27. Temperature Distributions at 10 Min. in Transient

Pipe L4 (k = 42, 50)



I = 4

Fig. 28. Temperature Distributions at 10 Min. in Transient



$K = 5$

Fig. 29. Temperature Profile at T1 Location

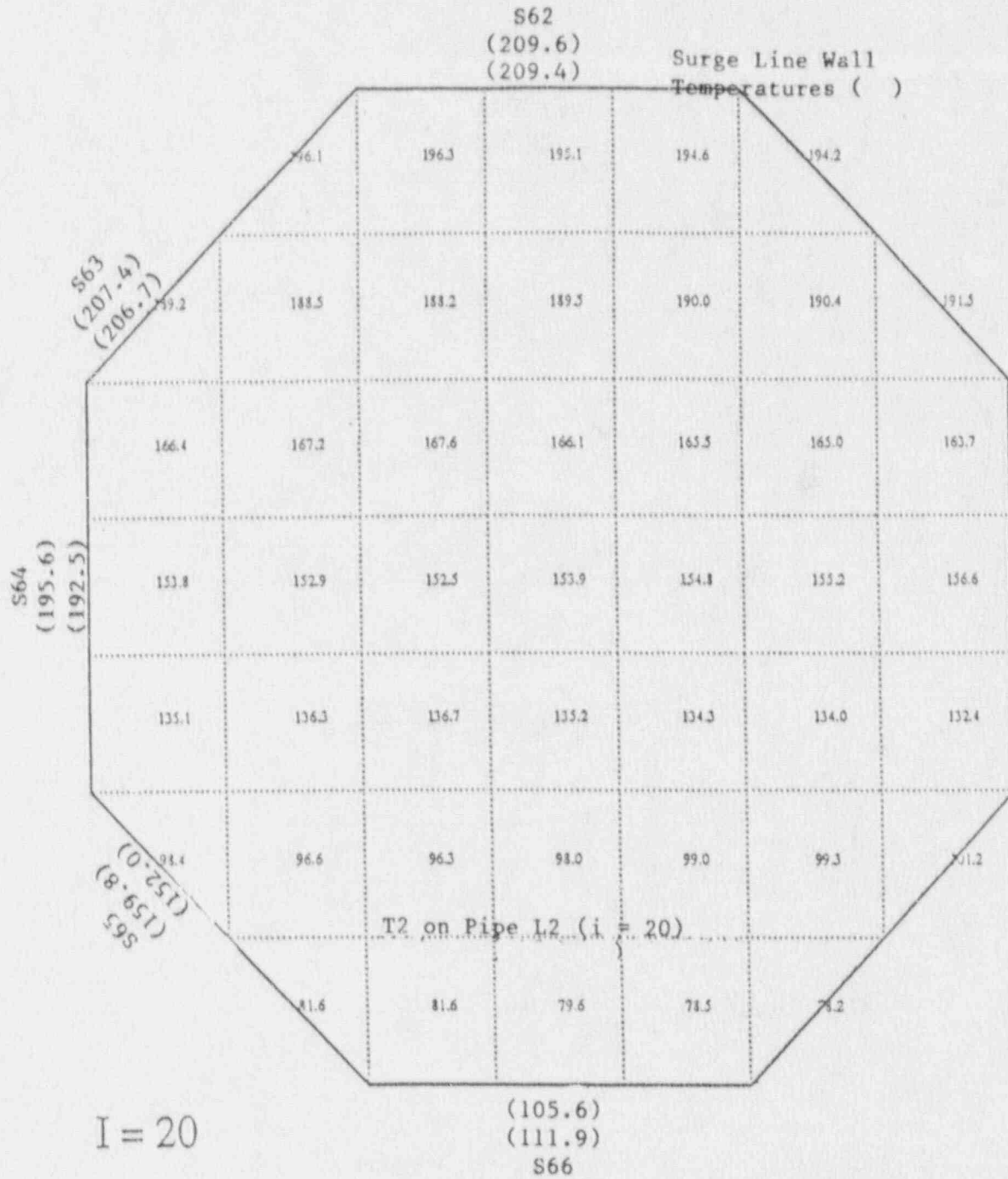


Fig. 30. Temperature Profile at T2 Location

DRAFT

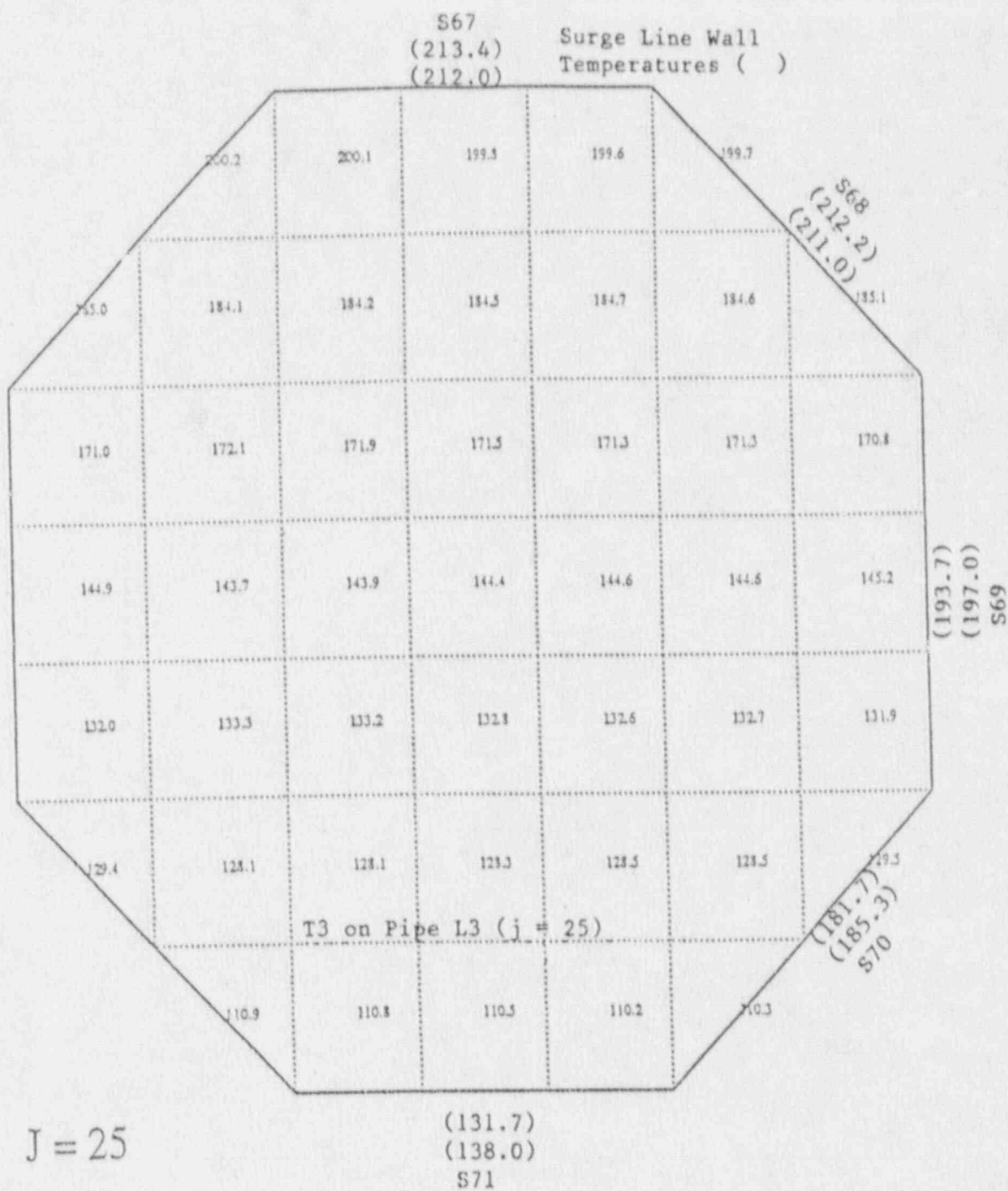


Fig. 31. Temperature Profile at T3 Location

DRAFT

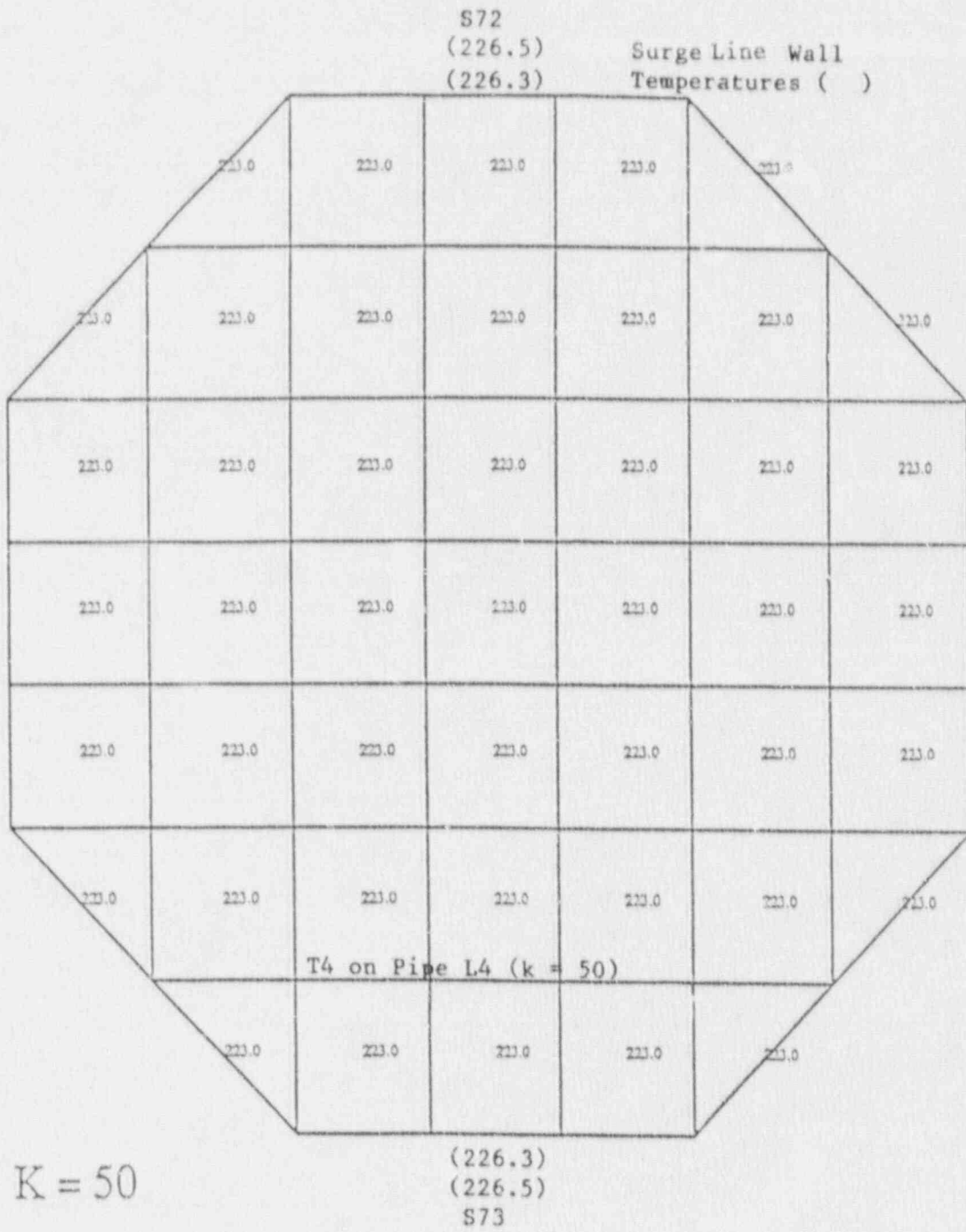


Fig. 32. Temperature Profile at T4 Location

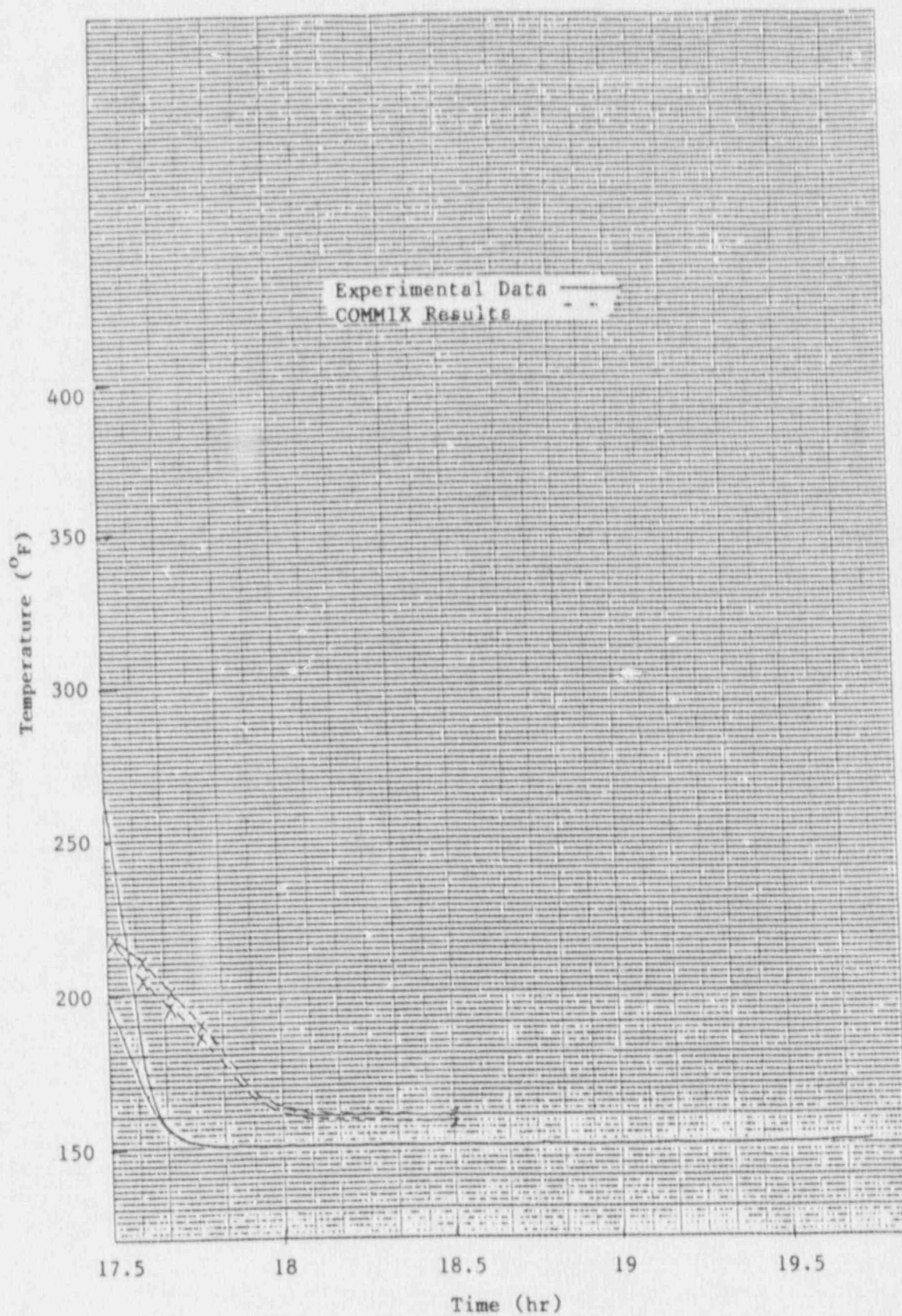


Fig. 33. COMMIX Results vs Experimental Data of T1

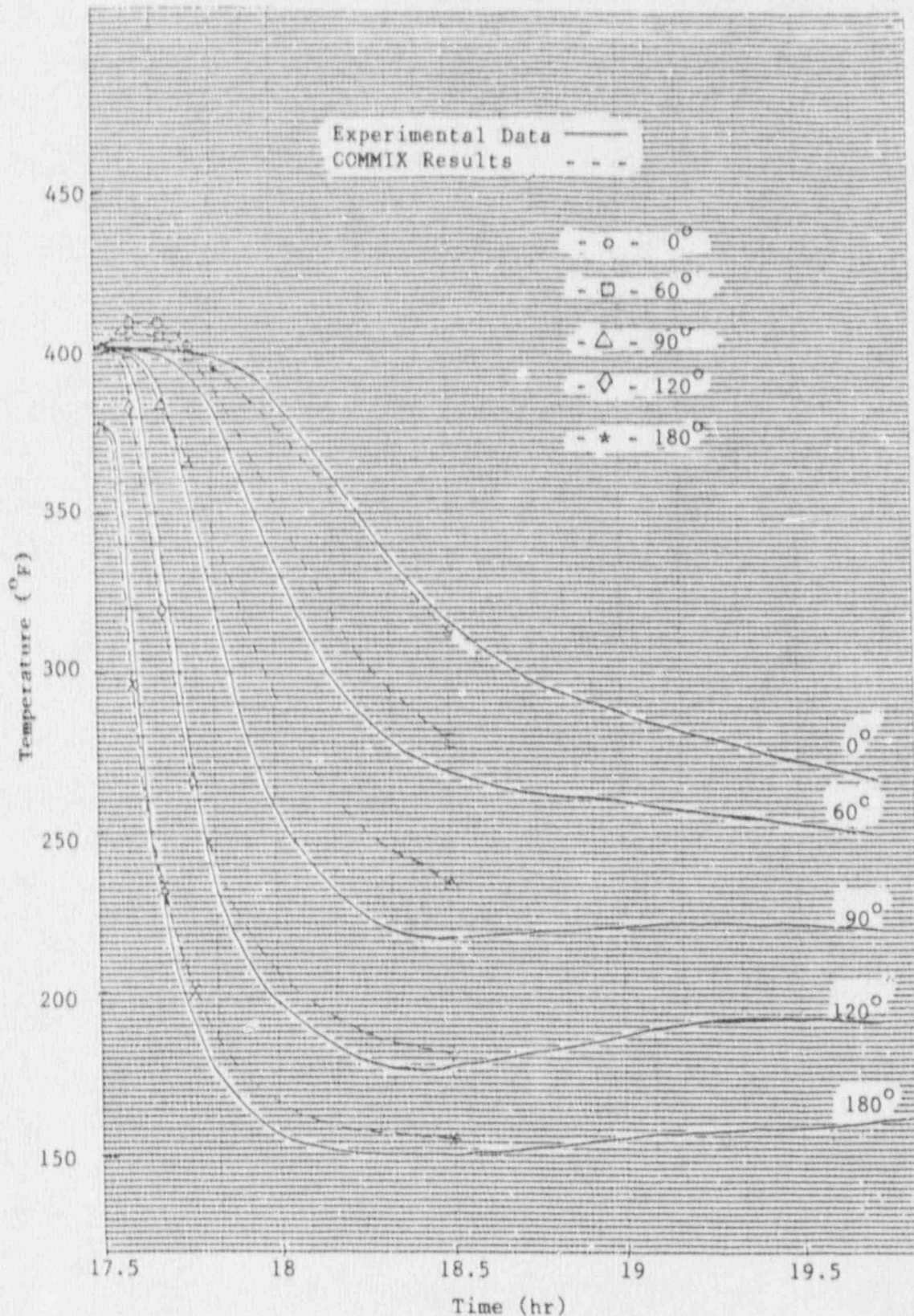


Fig. 34. COMMIX Results vs Experimental Data of T2

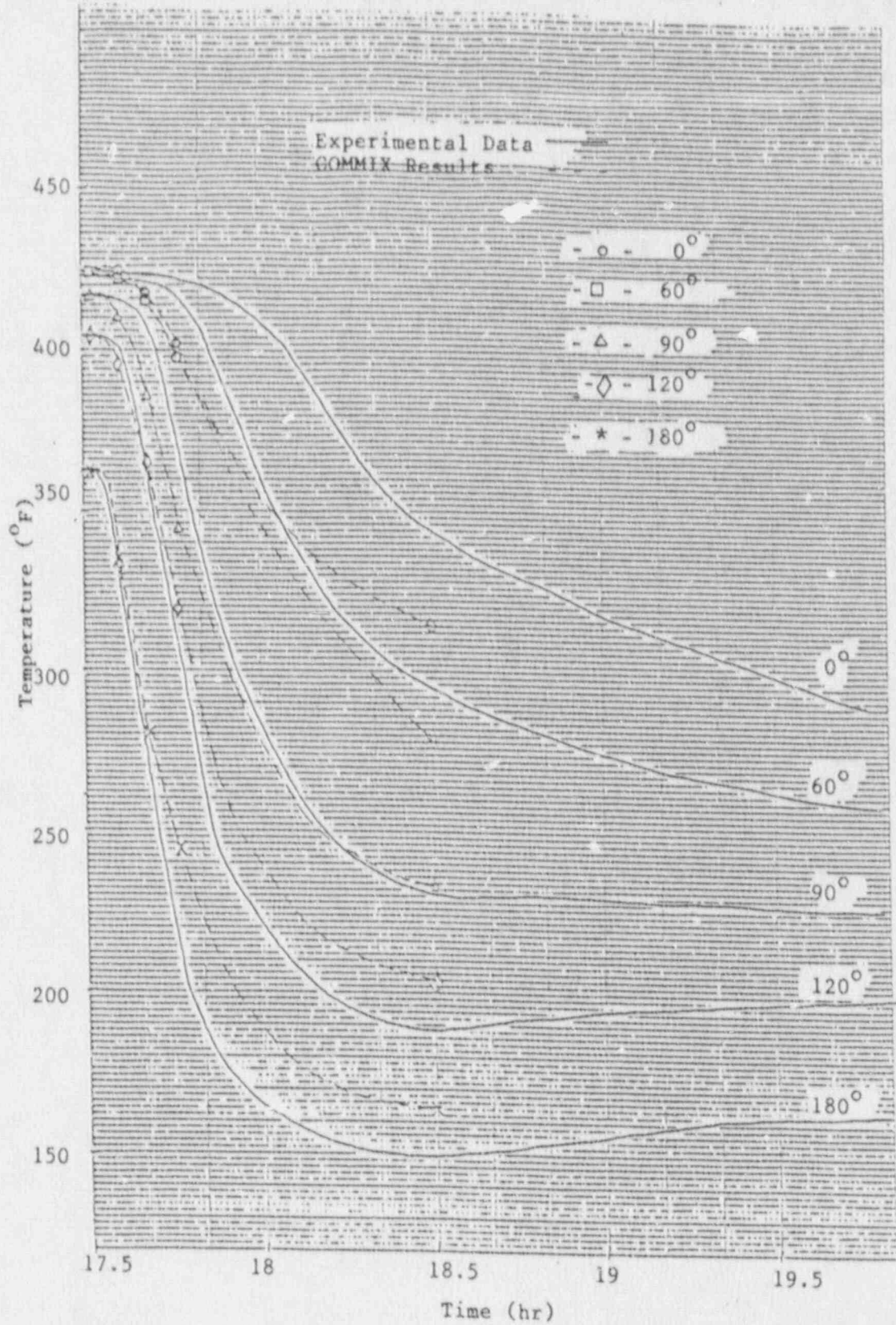


Fig. 35. GOMMIX Results vs Experimental Data of T3

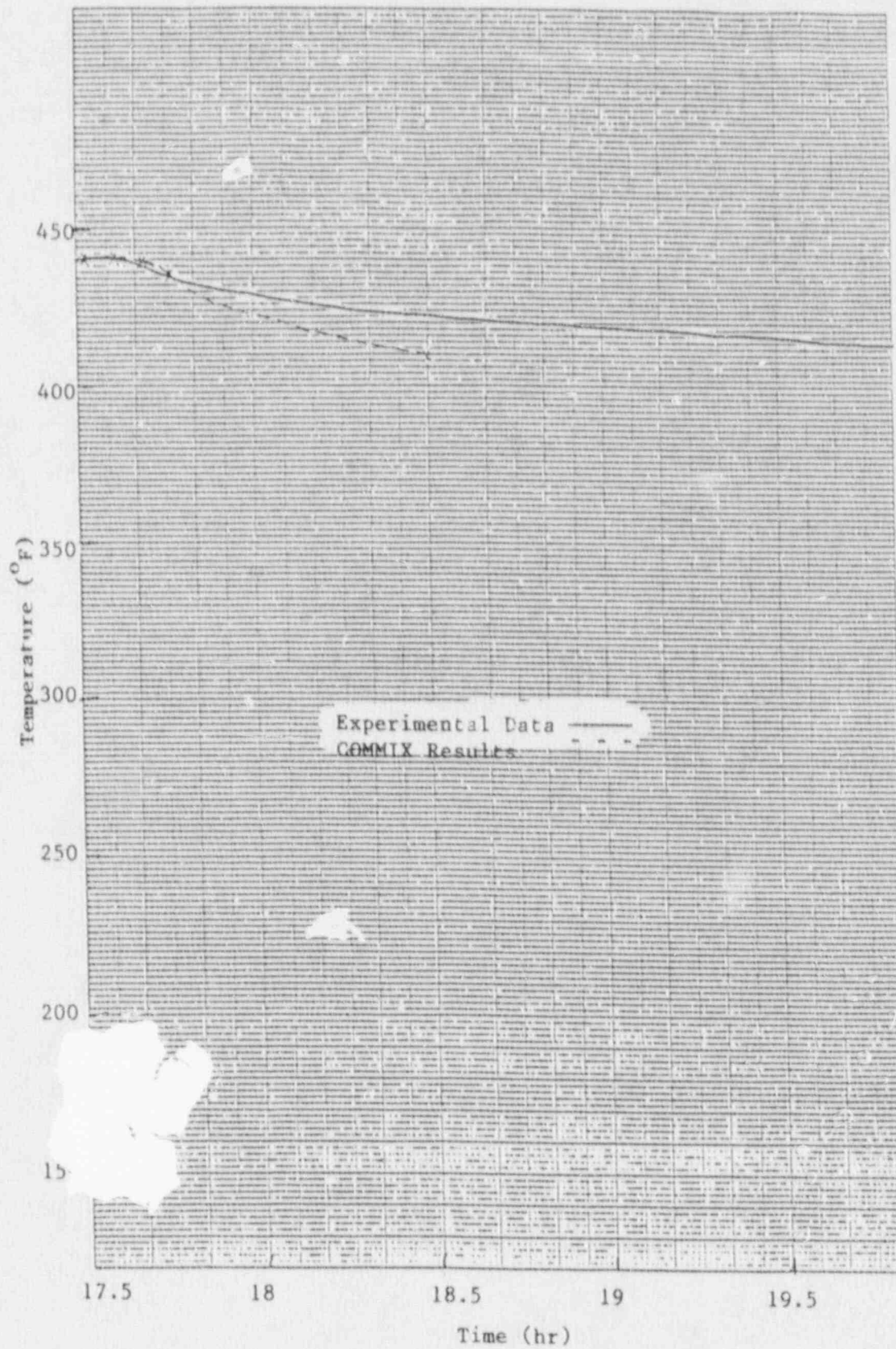


Fig. 36. COMMIX Results vs Experimental Data at T4